NASA Innovative Advanced Concepts (NIAC)

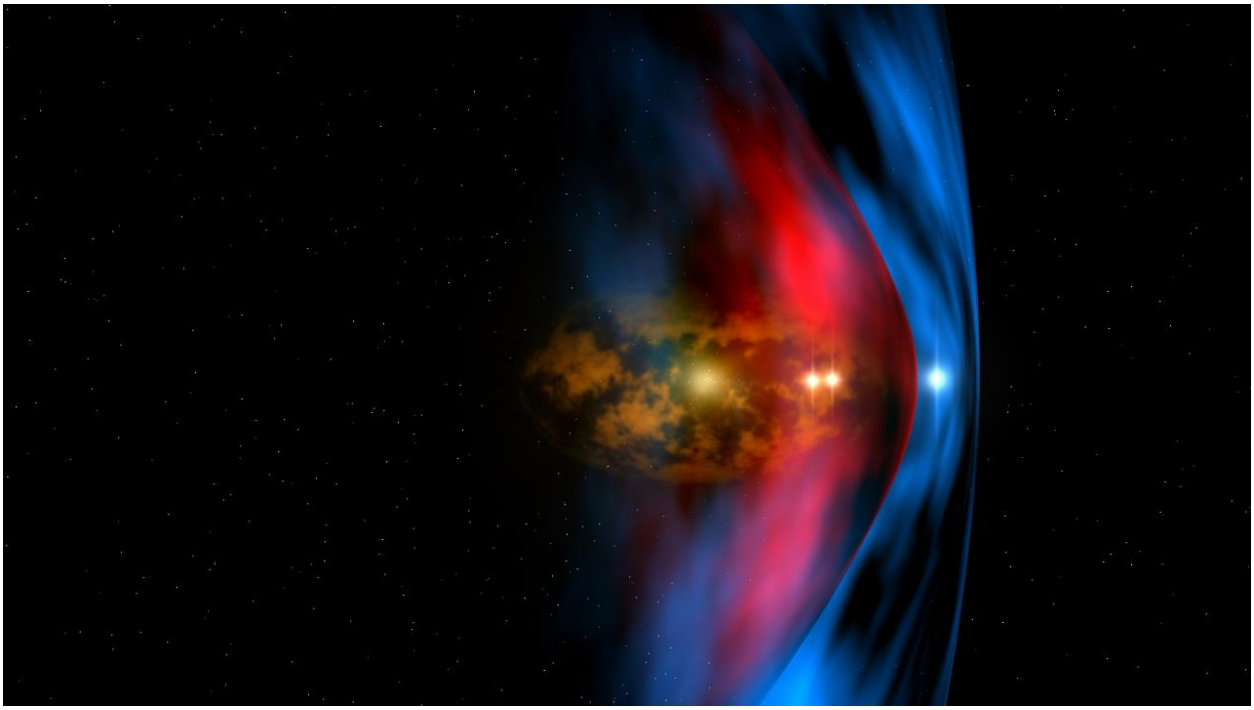

Heliopause Electrostatic Rapid Transit System (HERTS)

Final Report

14-NIAC14B-0075

April 27, 2015

Marshall Space Flight Center

Bruce M. Wiegmann, Principle Investigator

Table of Contents

List of Acronyms

ACO	Advanced Concepts Office
AU	Astronomical Unity
C&DH	Command and Data Handling
DSN	Deep Space Network
E-Sail	Electric Solar Wind Sail
FMI	Finish Meteorological Institute
FOV	Field of View
G&C	Guidance and Control
HGA	High Gain Antenna
HERTS	Heliopause Electrostatic Rapid Transit System
IBEX	Interstellar Boundary Explorer
IEMs	Integrated Electronic Modules
IIE	Innovative Interstellar Explorer
IHP	Interstellar Heliopause Probe
IMUs	Inertial Measurement Units
JGA	Jupiter Gravity Assist
KBO	Kuiper Belt Object
KISS	Keck Institute for Space Studies
LGA	Low Gain Antenna
LISM	Local Interstellar Medium
LMS	Langmuir Mott-Smith
MaSMi	Magnetically Shielded Miniature
MGA	Medium Gain Antenna
OML	Orbit-Motion Limited
PLF	Payload Fairing
RTG	Radioisotope Thermoelectric Generator
SRM	Solid Rocket Motor
SWF	Solar Wind Facility
TRL	Technology Readiness Level
TVC	Thrust Vector Control
TWTA	Travelling Wave Tube Amplifiers
USOs	Ultra-stable Oscillato
yr	Year

Introduction

This report represents a summary of the study conducted under NASA Innovative Concept study contract number 14-NIAC14B-0075. The report provides a summary of the results of all contracted tasks and provides a suggested roadmap for continued development. The effort was collaborated with the Finnish Metrological Institute on an unfunded basis and the results of that coordination are reported herein. The Heliopause Electrostatic Rapid Transit System (HERTS) provides a flexible and enabling technology that can accelerate a spacecraft to velocities that allow travel times on the order of a decade for reaching the Heliopause; a feat that took the Voyager spacecraft(s) over 30 years to perform. The propulsion system concept being described is faster than any current propulsion system under development by NASA. The report describes the mission, the propulsion concept, and solar system trajectories. It also provides a comparison to the current state of the art in advanced propulsion concepts.

Section 1: Executive Summary

The Electric Solar Wind Sail (E-Sail) is a revolutionary propulsion technology that uses the naturally occurring solar winds to produce thrust without the expense (mass) of propellants that enables trip times to the edge of the solar in half of the time as any alternative system. In addition to these benefits (reductions in travel times to solar system targets and launch costs) this system will enable qualitatively new types of non-Keplerian orbit missions. The E-sail taps the momentum flux of the natural solar wind for spacecraft propulsion with the help of long, positively charged wires (Figure 1). The system produces a thrust vector which points away from the Sun, but which can be turned at will within an approximately 30° cone and whose magnitude can be easily adjusted.

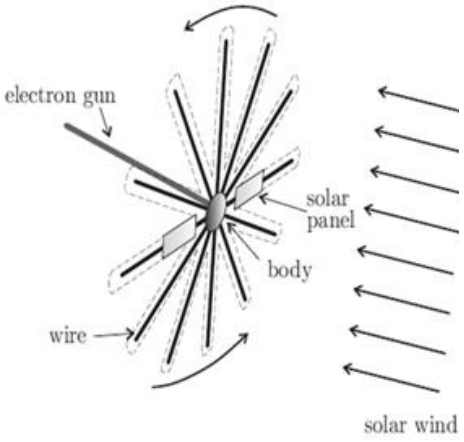

Figure 1: E-Sail model[1]

The electric sail design is a novel approach to solar propulsion. The thrust produced by an E-sail declines at a rate of $1/r^{7/6}$ (where r is the solar distance) and the system provides acceleration to distances of 30 AU. In comparison, the thrust of a solar sail propulsion system declines at a rate of $1/r^2$ and is only capable of accelerating a spacecraft to ~5 AU maximum[1].

An E-Sail mission to the Heliopause can be accomplished within 15 years[2] (Figure 2), a feat Voyager 1 took 29 years to accomplish. E-Sail velocities are 25% greater than solar sail options due to the

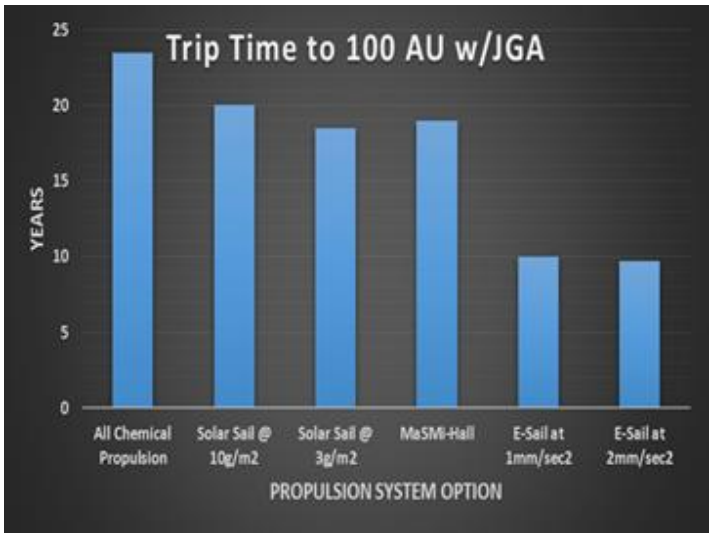

Figure 2: E-Sail technology reduces travel time to the Heliopause by a decade over current propulsion technology.

reduced rate of acceleration decline. E-Sail propulsion exceeds the 2012 Heliophysics Decadal Survey speed goal of 3.8 AU per year. Put in more human terms, the E-Sail technology will bring the time frame of Heliopause missions to well within a person's career. It may be difficult for a young researcher to decide to pursue a Heliopause mission with today's propulsion technology, knowing they may be at the end of a 30 year career before they see any results from the mission. E-Sail technology would supply results to an investigator with plenty of time to follow up with second or third missions that can build upon the conclusions and discoveries of previous missions.

Other possible applications of the E-sail include: An interstellar probe mission, multi-asteroid touring, Kuiper and Deep Space planetary or planetary moon flyby, a gas giant planet atmosphere probe, a 2-year sample return mission from Mercury, remote sensing of Earth, Sun and planets from non-Keplerian orbits. With these applications, the Electric Solar Wind Sail has the potential to qualitatively change space exploration and to unlock the scientific treasures of the solar system. [3]

Electric sail vehicles can enable missions outside the ecliptic and perform science in an orbit above the Sun by balancing a vectored thrust with the Sun's gravitational pull. Missions to Saturn and Jupiter can be accomplished in 1-2 years. Neptune and Uranus can be reached in 3-5 years. [4]

Because the E-sail can produce continuous thrust, it can be used to "float" a spacecraft against a weak gravity field on a non-Keplerian orbit (Figure 3). A probe could be set to orbit the sun in an orbit which is artificially lifted above the ecliptic plane. From such orbit there would be a permanent view to sun's polar region.

Because the E-sail thrust vector can be controlled in both magnitude and direction, it can be used to spiral inward or outward in the solar system by tilting the sail to brake or accelerate the spacecraft's orbital motion around the sun. E-sail enables arbitrary and rather fast transfers in the inner solar system as well as fast one-way trips to the outer solar system and beyond

Many asteroids are hard to reach with chemical rockets and ion engines. This is due to their low mass providing no gravitational slingshot effects and often significant orbital eccentricities and inclinations of the orbits. Because the E-sail can provide continuous thrust, it is very well suited for asteroid missions. An E-sail mission could make close inspection of 5-8 asteroids per year in flyby mode or 1-3 in rendezvous mode. [5]

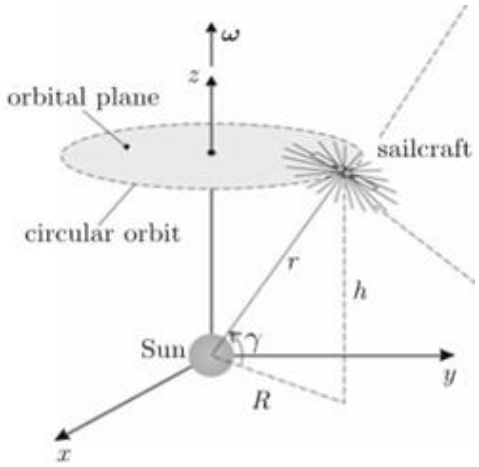

Figure 3: Example of non-Keplerian orbit above solar pole[4]

The E-sail can boost small and moderate mass spacecraft for outer solar system fly-by missions. Such probes could be launched flexibly, either together or as piggybacks with other missions because the E-sail is not delta-v limited. The flexibility of the concept, when successful, will enable a whole class of deep space exploration missions that saves large amounts of propellant mass. Any escape orbit launch can be used for launching any E-sail probe regardless of its target in the solar system. The E-Sail system is scalable and can enable a variety of mission classes from cubesats to larger New Horizons sized spacecraft.

An engineering team was assembled in 2014 to study the system as a whole and assess the technology of the required subsystems in order to craft a plan for future work. Current Technology Readiness Level

(TRL) on individual component technology (deployable wires, solar panels, electron gun, and satellite bus etc.) is generally 8 or 9 for each component, but when combined into the overall E-Sail system the TRL is very low due to the uncertainties dictating how each subsystem will interact with the others. The study was focused on identifying critical systems and components that will require immediate resources to increase the TRL of the total system. The team gave consideration to the possible requirements that might be levied on the E-Sail system to accomplish a mission to the Heliopause or to a destination outside the ecliptic based on the performance metrics outlined in the published papers of Dr. Pekka Janhunen of the Finish Meteorological Institute[6].

The team that was assembled to conduct this study was asked to consider the electric sail as a system, and identify the one or two most critical elements that their discipline would be asked to provide. Once all sub-system elements were identified, the team again assessed the system in its entirety. The discipline experts on the team chose the items they felt are the most critical for the system, and in need of the most resources to advance the cumulative TRL of the system. The group as a whole identified the systems most in need of development. The subsystems identified as high priority areas of research are:

Table 1: Critical subsystem identified by systems engineering design team in 2014

Sub-System	Level 1 Effort
*Wire Deployment	Trade space between chemical propulsion and electrical propulsion
Wire Configurations	Area optimization: how many wires vs length of wires
Wire Materials	Wire property requirements
*Wire Dynamics	Perform analysis
*High Voltage System	Wire voltage analysis
*High Voltage Switching	Trade between single power and multi power systems for the wires
*Momentum Management	Analysis of techniques to spin the system
*System Spin Propulsion	Trade methods of spinning the system
Attitude Control System	Develop system requirements for ACS prior to E-Sail deployment
Propulsion Performance	Analysis of various E-Sail configurations
Deep Space Comm	Develop requirements for deep space communications
Bus Accommodations	Concept design for E-Sail bus
*Electron Elimination	Develop requirements for electron elimination system
Electron Elimination Power	Analysis of power requirements

1) a deeper understanding of the physics behind proton interaction and the spacecraft;
2) the environment surrounding the elimination of electrons from the system;
3) guidance, navigation and control;
4) and the mechanical deployment of the wire sail.

Current level of effort is focused on the high risk areas denoted by an asterisk in Table 1.

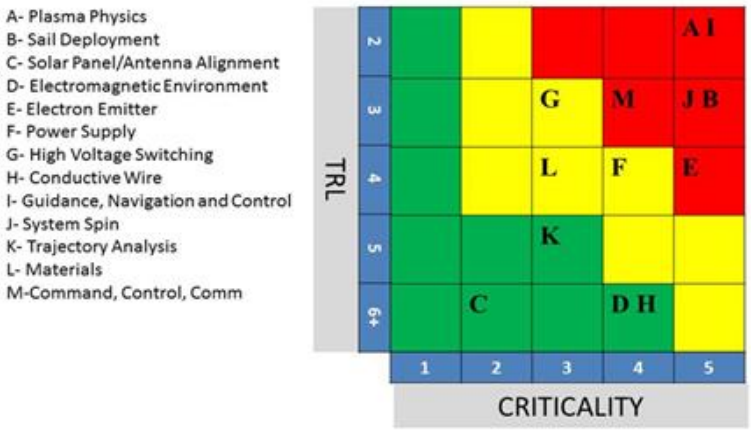

Figure 4: Subsystem criticality assessment

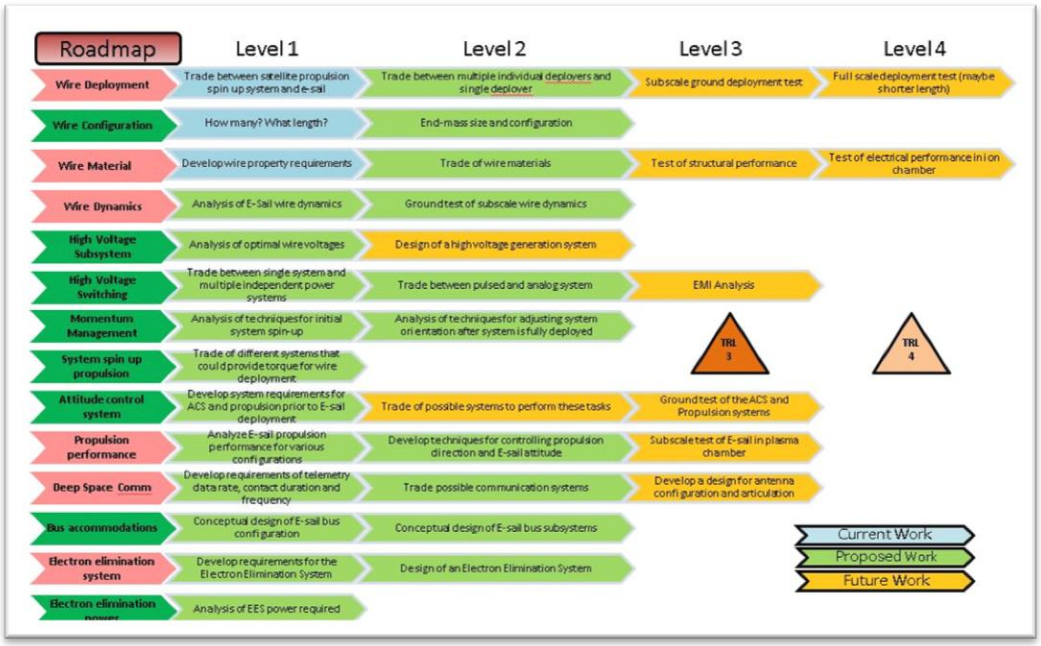

Figure 5: Roadmap

The team then ranked each subsystem by criticality to the system and overall TRL level as an integrated subsystem (Figure 4 and Figure 5). Recommendations were then provided for future work as shown in the level 1 effort in Table 1.

Section 1.1: HERTS/E-Sail Propulsion Concept

The E-sail is a revolutionary low-thrust advanced propulsion concept that is ideal for deep space missions to the outer planets, the Heliopause, and beyond. It is revolutionary in that it uses an E-Sail to

siphon momentum from the hypersonic solar wind and can provide propulsion throughout the heliosphere. Consistent with the concept of a "sail," no propellant is needed as electrostatic forces capture a small "push" from the solar wind that can, over a period of months, accelerate a spacecraft to enormous speeds—on the order of 100-150 km/s (~ 20-30 AU/yr).

The E-sail consists of 10-100 electrically conducting wire strands, each many kilometers in length. Strands are deployed from the main spacecraft bus and the spacecraft rotates to keep the strands taut. An electron gun is used to keep the spacecraft and the strands in a high positive potential. The electric field around the strands interacts with the solar wind, which is a plasma that flows radially away from the sun moving at speeds between 300 and 700 km/s. Momentum is transferred from the solar wind to the vehicle through the deflection of the positively charged solar wind protons by a high voltage potential applied to the wires.

Unlike other propellantless concepts, the electric sail does not rely on a fixed area to produce thrust. In fact, as the electric sail moves away from the sun, the electron Debye length decreases and causes the positive electric field to grow, increasing the apparent area of the virtual sail. This results in thrust decreasing as $\approx 1/r^{7/6}$ instead of the $\approx 1/r^2$ relationship typical of a solar sail [7].

The magnitude of the total thrust generated is related to the effective cross-sectional area over which the solar wind is perturbed. This is proportional to the total length of the wires, but it also is highly dependent on the efficiency of the interaction between the biased wires and the solar wind. The wires themselves are less than 0.1 mm in diameter. However, the effective radius—the range of the imposed electric field—is much greater. This range is characterized by a proton impact parameter, P, which is directly proportional to the magnitude of the applied positive potential and the Debye shielding distance, λ_D, of the solar wind plasma ($\lambda_D \approx T_e^{1/2}/n_e^{1/2}$,where T_e and n_e are electron temperature and density, respectively). The total force on the wire array is given by:

$$F = m_P n_P v_P^2 N_W P(\phi, \lambda_D),$$

where; m_P, n_P, and v_P are proton mass, number density, and velocity; N_W and L_W are the number and length of the wires; and ϕ is the electrical bias on the wire. Therefore, as the vehicle moves away from the sun and the solar wind density decreases (as $1/r^2$, where r is the radial distance from the Sun) the proton impact parameter increases – which helps maintain the thrust level and compensates for the reduced plasma pressure.

The important components of the propulsion system are the wire array, kept in tension by a slow rotation; a wire deployment system; an electron gun to maintain the positive bias on the wires; a programmable high-voltage power supply; and a power distribution system. The bias of each wire must be individually controlled through the use of a power distribution system to enable thrust vectoring. Critical wire design parameters include material, diameter, total length, count, electrical bias, and configuration (single vs. multiple strand and geometry).

Speeds in excess of 50 km/s (10.5 AU/yr) are predicted in early calculations by Quarta and Mengali [2]. A NASA technical paper by Stone[8] includes experimental data which was used to calculate a thrust approximately 3.5 times higher than previous calculations by Pekka Janhunen[7]. The difference can be resolved through additional testing in the MSFC Solar Wind Facility (SWF) under realistic solar wind conditions that will be accomplished under the Phase II portion of the NIAC award.

This concept is very flexible and adaptable. The previously discussed parameters allow the mission/vehicle designers to trade off wire lengths, number of wires, and applied voltage levels to determine sensitivity variations for the integrated spacecraft design. The bias of the wires can be modulated as the vehicle rotates to provide thrust vectoring over a wide angle range. This provides for mission concepts that involve visits to multiple planets or objects of interest within the solar system.

Additionally, the wire array structure may provide benefits in addition to propulsion. Feedback from the wires may provide information about the structure of the solar wind and it is hypothesized that the

array may also be utilized to supplement communications. As an example, individual wires may be biased and modulated such that they act as a large phased array RF antenna, increasing communications range, bandwidth, and reducing power requirements. Also, individual wires may act as a long Langmuir probe, capable of measuring spacecraft floating potential, electron density, and temperature of the deep-space plasma environment.

The propulsion system can be sized anywhere from cubesats to large scale spacecraft. However, the system is not effective within the magnetosphere of a planet due to reduction in the solar wind; it is only useful for interplanetary missions. Also, the effectiveness of the sail drops as it approaches the sun due to the decreased Debye length effects; it is perfectly matched for 0.5 AU and greater missions.

Current Technology Readiness Level (TRL) on individual component technology (wires, solar panels, electron gun, and satellite bus) is generally 8 or 9, but when combined into this system the TRL is 2. This effort was intended to identify critical systems and components that will require immediate resources to increase the TRL of the total system to TRL 3 or 4.

The electric sail technology has the potential to open new areas of scientific research, and these abilities were taken into consideration during this study. For example, this technology has the potential to fly payloads out of the ecliptic and into other non-Keplerian orbits, place payloads in a retrograde solar orbit, flyby missions to terrestrial planets and asteroids and position instruments for off-Lagrange point space weather observation. It is a low mass/ low cost propulsion system. Electric sail thrust decays at a slower rate than solar sail thrust. Solar sails produce thrust up to 5 AU, whereas this electric sail produces thrust up to 30 AU. This technology enables 10-15 year missions to the Heliopause. The team gave consideration to the possible requirements that might be levied on this system to accomplish such missions.

Section 2: Study Purpose

The motivation for advanced heliospheric propulsion technology comes from the 2013 NASA Heliophysics Decadal Survey. Section 10.5.2.7 states, in part; ***"recent in situ measurements by the Voyagers, combined with all-sky heliospheric images from IBEX and Cassini, have made outer-heliospheric science one of the most exciting and fastest-developing fields of Heliophysics".*** The Decadal Survey goes on to say, ***"The main technical hurdle is propulsion. Advanced propulsion options should aim to reach the Heliopause considerably faster than Voyager 1 (3.6 AU/year)". The Solar and Heliospheric Physics (SHP) Panel placed high priority on NASA developing "the necessary propulsion technology for visionary missions like The Solar Polar Imager (SPI) and Interstellar Probe to enable the vision in the coming decade".*** The flight duration of a Heliophysics missions only allows for one experiment within the professional lifetime of a scientist; reducing the time to around a decade would allow for multiple experiments within their lifetime.

The issues identified in Phase I as high priority for the proposed Phase II study are:

1. Lack of a reliable model for solar wind proton and electron interactions with the highly biased wires.
2. Injection of collected solar wind electrons back into space.
3. Deployment of charged wires and investigation of wire dynamics.
4. Guidance, navigation and control using voltage control on the individual wires of the array.

2.1 Mission Concept and Purpose

The HERTS is a revolutionary propulsion concept that is ideal for deep space missions to the outer planets, the Heliopause, and beyond. It is revolutionary in that it uses an E-Sail to obtain momentum from the hypersonic solar wind and can provide propulsion throughout the heliosphere (shown schematically in Figure 6). Consistent with the concept of a "sail," no propellant is needed as electrostatic interactions capture a small amount of thrust from the solar wind that can, over a period of months, accelerate a spacecraft to enormous speeds—on the order of 100-150 km/s (~ 20-30 AU/yr). ***Accordingly, the HERTS would enable a spacecraft to reach the Heliopause in less than 15 years.***

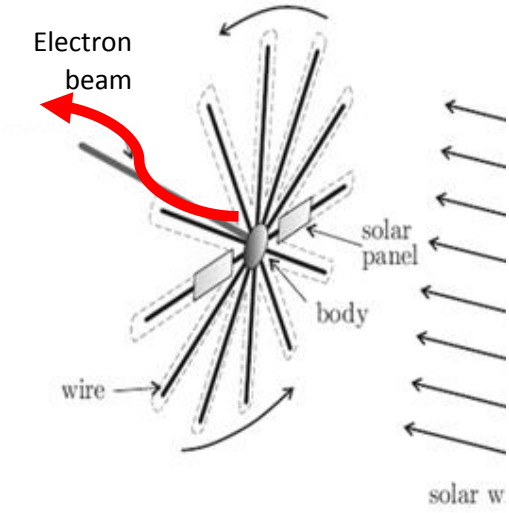

Figure 6: E-Sail model with electron beam

The basic principle on which the HERTS propulsion system operates is the exchange of momentum between an "electric sail" and solar wind, which continually flows radially away from the sun at speeds ranging from 300 to 700 km/s. The "sail" consists of an array of long, charged wires which extend radially outward 10 to 30 km from a slowly rotating spacecraft (see Figure 6). Momentum is transferred from the solar wind to the array through the deflection of the positively charged solar wind protons by a high voltage potential applied to the wires.

E-Sail propulsion has been explored and recently published in the open literature—primarily by Dr. Pekka Janhunen of the Finnish Meteorological Institute (FMI) [7,10]. The MSFC Advanced Concepts Office (ACO) performed a top level feasibility study in 2013 that indicated a HERTS can accelerate a spacecraft to velocities as much as three to four times that predicted by any realistic extrapolation of solar electric and solar sail propulsion systems. The results of the Phase I NIAC study found the concept to be feasible from a mission design perspective and identified technical issues for further study. Since most of the E-Sail propulsion system components already have a flight heritage, it can be reasonably expected that a HERTS system—capable of reaching the Heliopause in less than 15 years—could be developed within a decade and provide meaningful Heliophysics Science in the 2025-2030 timeframe. Further the propulsion system can be used to explore any of the major planets or their moons with transit times significantly less than any other concept.

2.2 Interaction with Solar Wind Protons

The total force on the wire array can be represented by:

$$F = m_p\, n_p\, v_p^{\,2}\, N_w\, L_w\, P(\varphi_w, \lambda_D)\ ,$$

Where: m_p, n_p, and v_p are proton mass, number density and velocity; N_w and L_w, the number and length of individual wires. The effective radius of the biased wire is characterized by the proton impact parameter, P_+, which is proportional to the magnitude of the applied positive potential, φ_w, and the Debye shielding distance, λ_D, of the solar wind plasma ($\lambda_D = 6.9\ (T_e/n_e)^{1/2}$ cm, where T_e is electron temperature is ^oK and n_e is the number of electrons per cm^3). Protons that enter the sheath and pass within a distance $r = P_+$ of the wire will be deflected significantly and contribute to a reactive force on the wire which is directed radially away from the sun (parallel to the solar wind flow). Those that pass outside of $r = P_+$ will not be

significantly disturbed. Therefore, P_+ determines the effective radius of the wire for protons (Figure 7, red trajectories).

In the Phase I study, P_+ was approximated by an extrapolation of plasma chamber data taken in a previous MSFC study of the interaction of orbiting spacecraft with the ionospheric plasma [8]. Because ionospheric satellites are typically biased a few volts negative, these experiments involved attractive potentials that deflected the streaming ions toward the test body. However, because differential measurements of ion flux (direction and intensity) were made [10], the flux angle at the measurement point downstream could be extrapolated back up stream to the point of deflection in the sheath of the body (spheres and short cylinders were used). In this way, the impact parameter, P_+, was determined to be:

$$[P_+/\lambda_D] = 6.87\,[\Phi_w/S],$$

where λ_D is the Debye Length; $\Phi_w = (e\varphi_w/kT_e)$ is the normalized potential where e is the electronic charge and k is Boltzmann's constant; and $S = (m_p v_p^2/2kT_e)^{1/2}$ is the ion acoustic Mach number. Taking nominal solar wind parameters at 1AU ($T_e = 1.5\text{x}10^5$ °K; $n_e = n_p = 7\text{x}10^6$ m^{-3}; and $v_p = 400$ km/s) we have

$$P_+ = 8.6\,\varphi_w^{1/2};$$
$$A_w = 2\,P_+(\varphi_w)\,L \text{ (area per wire); and}$$
$$f_p = n_p m_p v_p^2 = 1.89\text{x}10^{-9} \text{ N (solar wind proton pressure per } m^2).$$

with engineering parameters L = 30 km and φ_w = 6,000 volts, we have P_+ = 669 m, and $A_w = 4\text{x}10^7$ m^2. The force generated per wire is then, $F = f_p A_w$ = 76 mN.

Note that in this analysis, it was assumed in using the plasma chamber test data that the impact parameter for an attractive potential is the same as that for a repulsive potential and that body geometry does not have a major effect. While these appear to be reasonable assumptions, because an accurate determination of P_+ is critical to determining reliable thrust values, the first objective of the experimental plasma chamber tests proposed for Phase II will be to validate these assumptions by performing a similar set of measurements with a repulsive (positive) potential applied to a long cylindrical test body that is more representative of a long wire.

2.3 Interaction with Solar Wind Electrons

In 1924, Irvin Langmuir and H. M. Mott-Smith published the theoretical LMS model for electrostatic probes [11] (subsequently known as Langmuir probes). Although the Langmuir probe is physically simple (a biased wire) the theory describing its functional behavior and its current-voltage characteristic is extremely complex, requiring simplifying assumptions to obtain a tractable problem. These simplifying assumptions, correspondingly, place limits on the range of application of the model. One of these simplified treatments; the Orbit-Motion Limited (or OML) model, forms the basis for previous calculations of the current that should be collected by the long, biased wire of an E-sail. We must, therefore, pay attention to the inherent assumptions and limitations of the theory when relying on it for E-sail design parameters. This situation is briefly described below.

2.4 General Description of the LMS Model

In the vicinity of a boundary the conditions that define plasma, such as quasi-neutrality, may break down. For example, an electrically biased surface can form a boundary layer as one species is preferentially absorbed at the surface and quasi-neutrality no longer holds in the neighboring region. The plasma, in turn, tends to be shielded from the boundary and its potential by this charge-rich layer—called the "plasma sheath." The sheath can support substantial electric fields as the boundary potential is matched to the plasma potential (which we

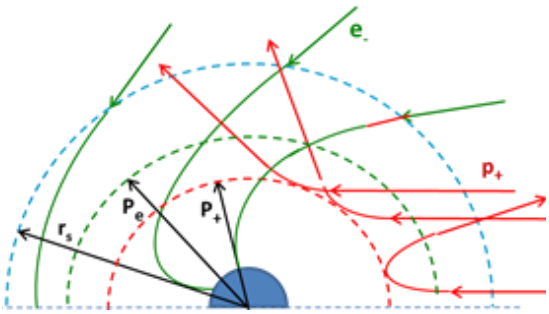

Figure 7: Proton and Electron Trajectories in a High Voltage Sheath

will assume to be zero).

The LMS identified some very special cases (applicable to a number of cases of interest; e.g., electrostatic probes in laboratory plasma) which greatly simplified the problem, allowing a closed form solution. For an infinite cylinder this theory results in a simple expression for collected electron current of the form:

$$I = A_w j_{eo} P_e, \tag{1}$$

Where: j_{eo} is the solar wind electron thermal current (outside the sheath), P_e is the electron impact parameter, and j_{eo} is the average current density for a Maxwellian (equilibrium) electron distribution, given by:

$$j_{eo} = \frac{e n_e}{4}\left(\frac{8kT_e}{\pi m_e}\right)^{\frac{1}{2}}. \tag{2}$$

The parameter, P_e is a simple means of determining which electrons will hit the wire; i.e., all electrons that enter the sheath and pass within a distance $r = P_e$ are assumed to contact the wire and be collected, while those that enter the sheath but pass outside of $r = P_e$ are assumed to escape—as shown in Figure X, (green trajectories). The effective collection surface for electrons is, therefore, defined by $r = P_e$, rather than $r = r_w$.

Determining P_e for a thermalized plasma, requires integrating the electron velocity distribution, *f(u,v)*, which is a rather complicated process carried out in Huddlestone.[12] Assuming a *thick sheath* ($r_s >> r_w$) and high voltage ($\Phi_w >> 1$) leads to

$$P_e \approx \frac{2}{\sqrt{\pi}} {\Phi_w}^{1/2}, \tag{3}$$

and substituting expressions (2) and (3) into Equation (1) for the collected current gives:

$$I_e = \frac{e n_e}{\pi} A_w \left(\frac{2e\,\phi_w}{m_e}\right)^{\frac{1}{2}}. \tag{4}$$

Equation (4) is precisely the expression that has been used to calculate the magnitude of the electron current collected by the highly biased wires of an E-Sail. It cannot be too strongly emphasized that, because this expression is derived from the LMS formulation, the results obtained are subject to all of the limitations inherent to the LMS model.

2.5 Effects of the Assumptions

The LMS treatment, from which the OML model is derived, assumes that there are no collisions in the plasma on the scale of the electrode, Maxwellian electrons, a monotonically decreasing potential in the sheath, total absorption of all electrons that contact the electrode; no collisional effects; no ionization of neutrals; no recombination of charged particles to form neutrals; no photo-emission from the electrode surface; no magnetic field effects; and quasi-static conditions (no bulk drift of the plasma). Clearly, many of these conditions will be violated in the E-Sail application and can introduce significant uncertainty and error into calculations of the collected electron current. For example:

(1) ***No collisional effects.*** This requires collected electrons to undergo free molecular flow so that their trajectories through the sheath region are determined totally by the sheath electric field. While the Solar Wind can be considered collisionless on the scale of the sheath, this condition may not hold within the sheath where the electric field will focus the electron flux crossing a large surface area into a small volume, thereby raising the density. This has been observed in experimental investigations of the behavior of ions in attractive sheath fields around cylindrical and spherical bodies—and the focused ion fluxes are observed to interact. Electron fluxes would be expected to exhibit a similar behavior. [4]

(2) ***All contact electrons are collected.*** However, electrons passing within $r = P_e$ may also go into orbit around the wire and become trapped. Again, this effect has been observed for the case of

ions. Trapping will result in the build-up of a negative space charge and can cause a non-monotonic potential distribution, neither of which is accounted for in the OML model.

(3) ***Quasi-static conditions.*** This requires plasma drift motion to be small wrt the thermal motion of the plasma constituents—and this is not the case. The Solar Wind has a very large drift velocity—from which we propose to extract momentum to produce a propulsive force.

The OML model cannot be relied on until, and if, it is found be insensitive to the violations of its underlying assumptions that are unavoidable in E-Sail applications. We, therefore, propose to adapt a more powerful numerical particle-in-cell (PIC) model to the E-Sail application and first apply it to a case that can be simulated in the MSFC plasma chamber—much like the above test proposed to validate P_+. The experimental results will provide bench-mark data with which the numerical model can be validated. The numerical model can then be applied to conditions appropriate for an E-Sail in the solar wind (not generally achievable in plasma chambers) and used to derive reliable engineering parameters required for a HERTS preliminary design (i.e., voltage, power, and wire length requirements and corresponding thrust generation levels).

Section 3: Notional Spacecraft

Constructing a spacecraft to fly a mission to the heliopause within 15 years brings up a number of unique issues in spacecraft design. One of the biggest issues is the power source, as the vehicle will travel far beyond the range where the sun may provide significant solar power; because of this, the thermal environment will be of primary consideration. Power supply can be accomplished by the use of a Radioisotope Thermoelectric Generator (RTG). Thermal management can be accomplished by the balanced use of thermal blankets and waste heat generated by the RTG. Telemetry time to and from Earth will increase with distance, and dictate software requirements for spacecraft autonomy. The electric sail spacecraft will need to draw on the successful designs of similar craft that have journeyed to the depths of the Solar System. The most recent spacecraft in this class of vehicle is New Horizons, which was designed based on previous spacecraft such as Ulysses. The electric sail spacecraft will draw heavily from the New Horizons[13] design and incorporate New Horizons lessons learned.

3.1 : Spacecraft w/o the Propulsion System

3.1.1 Mechanical Configuration

The primary function of the spacecraft bus will be to house, deploy, and control the wires used for electric sail propulsion. Current preliminary designs dictate that the craft must rotate in order to keep the wires taut. New Horizons was similarly designed to use rotation for stability and antenna orientation to Earth.

Some New Horizons top level requirements were:

1. A configuration that aligns the principal moment of inertia axis with the High Gain Antenna (HGA).
2. Placement of the single RTG in the X-Z plane of the spacecraft to increase the angular momentum and maximize the distance of this source of radiation from the electronics and instruments.

The electric sail spacecraft will require mechanisms designed to deploy the propulsion wires up to ten kilometers, and an electron gun to strip electrons from the wires and eject them from the system in order to maintain the positive electrical bias required to interact with the solar plasma.

3.1.2 System Configuration

New Horizons provides multiple layers of redundancy with two Integrated Electronic Modules (IEMs). Each IEM contains: a Guidance and Control (G&C) processor; RF electronics for communication; a Command and Data Handling (C&DH) processor; and a 64 GB solid state recorder. Block redundancy is present in many of the remaining systems including star trackers, and Inertial Measurement Units (IMUs). System reliability is improved by the use of significant cross-strapping below the block level. The electric sail vehicle will benefit from similar redundant designs.

3.1.3 Propulsion Subsystem

The propulsion system for the electric sail vehicle will be unique and will not draw from the design of New Horizons. However, there may be secondary propulsion required that may be derived from other spacecraft designs as needed.

3.1.4 Guidance and Control

The electric sail spacecraft will have a very large moment of inertia due to the nature of the main propulsion system. The guidance and control systems will be unique to the spacecraft and will not be derived from New Horizons. However, similar sensors to determine attitude may be employed, including star trackers, IMUs and sun sensors. A high degree of spin axis knowledge will be required for the electric sail vehicle, which is similar to New Horizons requirements. New Horizons is capable of providing spin axis attitude knowledge of the spacecraft to better than +/- 471 micro-radians 3 σ and spin phase angle knowledge within +/- 5.3 milli-radians 3 σ.

3.1.5 Communication System

The electric sail spacecraft will require telecommunication systems similar to New Horizons. New Horizons uses the Deep Space Network (DSN) and a communications system that consists of an antenna assembly, Travelling Wave Tube Amplifiers (TWTAs), Ultra-stable Oscillators (USOs) and redundant uplink and downlink cards. New Horizons uses Medium Gain Antenna (MGA), Low Gain Antenna (LGA), and HGA. The MGA allows for communication at angles up to 4 degrees difference between the +Y axis and Earth, and is viable up to 50AU. The HGA provides communication within 0.3 degrees deviance of the +Y axis and Earth, and is capable of transmitting 42 dBic gain, 600 bps downlink at 36 AU. The electric Sail will travel to the heliopause, which is 121 AU from the sun, so further communications considerations will need to be made for the electric sail vehicle.

3.1.6 Thermal Management

The New Horizons spacecraft uses thermal blankets and the waste heat from the RTG to regulate the thermal requirements of the system. Thermal louvers on the lower deck of the spacecraft are used and excess electrical power is dissipated either internally or externally. The avionics are contained within a double wall design insulator within the spacecraft bus. The electric sail spacecraft will benefit from similar thermal design solutions.

Section 3.2: E-Sail Propulsion System – Wire & Wire Deployers Subsystem

One aspect of the phase I study was to examine how an E-Sail propulsion subsystem might impact the overall configuration of a deep space vehicle. The team used the New Horizon spacecraft as a baseline as discussed above and added the E-Sail propulsion system to the current configuration (Pluto mission) to examine how the vehicle would need to be reconfigured to allow the use of the E-Sail concept. The figures below represent an initial look at how that particular vehicle would have been impacted. The spacecraft is spin stabilized during flight and the E-Sail propulsion subsystem has been mounted on the centerline of the vehicle spin axis. Of course the various sensors and other appendages on the surface of

the vehicle must be relocated to ensure clearances for the wires. This is a top-level assessment so the relocation of these sensors was assumed to be a minimal impact to the mission. No changes were made to the spacecraft on board propulsion systems so this approach would result in duplicate propulsions systems. Obviously the vehicle designers would take advantage of this and use the volume and mass for other functions or eliminate them to reduce vehicle volume and mass.

The resulting configuration appears to show only minimum impact to the vehicle configuration. This is very encouraging and implies that the E-Sail could be configured as a bolt on subsystem allowing the vehicle designers a great deal of flexibility. The particular configuration shown reflects the counter rotating momentum devices but a second configuration was examined with the rocket deployment system that occupied the same volume of the second momentum wheel.

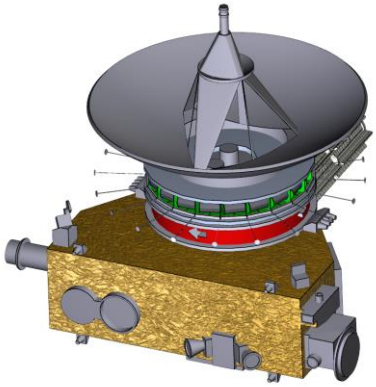

Figure 9: New Horizon spacecraft with an E-Sail propulsions system mounted below the antenna system

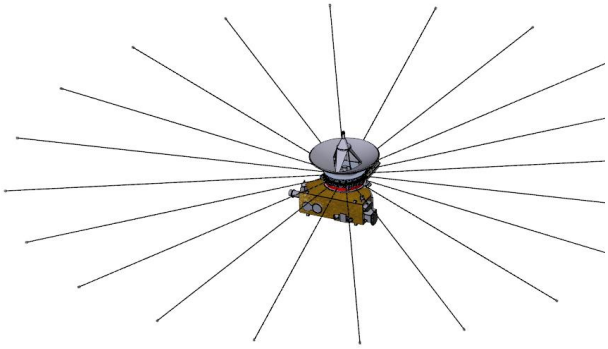

Figure 8: New Horizons Spacecraft with wires partially deployed

The following figures show how the vehicle configuration will work with the rocket deployment system. Again the basic configuration is very similar to the one shown above but now two small rockets are used to deploy groups of wires and then the rockets are used to fan out the wires.

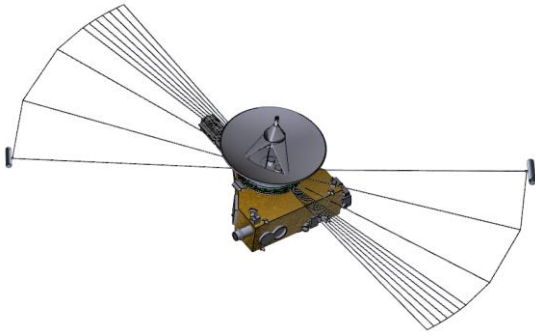

Figure 11: Vehicle configuration is shown with the rocket deployment system

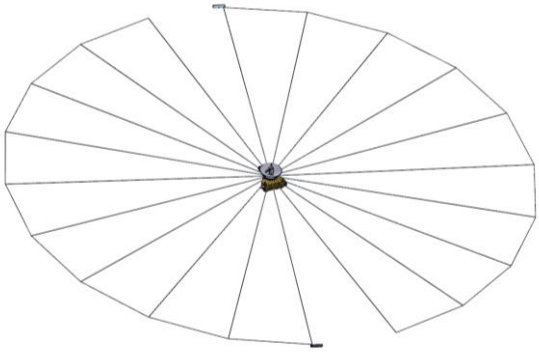

Figure 10: Vehicle configuration with wires deployed

3.2.1 Wire Concept

3.2.1.1 Strength and Conductivity:

The wire structures for the E-Sail are conductive wires or conductive fibers deployed from the spacecraft. A multi-kilovolt positive bias potential is applied to the wires so as to create a large electrostatic plasma sheath around the wires that reflects solar wind protons, thereby generating a thrust force on the wire. The positively biased wires will collect electrons from the solar wind plasma, and therefore must provide sufficient conductivity to conduct the electrons to the central spacecraft with a minimal potential drop so that the outer portions of the wires remain biased at a multi-kV potential with respect to the solar wind plasma. The wires must also have sufficient tensile strength to support both the electrostatic thrust and the centrifugal forces on the wire due to rotation of the system, and the thrust achievable by the E-Sail scales proportionally with the wire structure's tensile strength[14]. Although the desires for conductivity and strength argue for large-diameter wires, these drivers must be balanced with minimizing the mass of the E-Sail as well as minimizing the power required to sustain the bias voltage. Because the thrust generated scales only very weakly with conductor diameter while the bias power required scales with the the wire diameter and the mass scales with the square of the diameter, maximizing system performance requires using the minimum possible wire diameter with a material that provides the best balance between conductivity and strength.

3.2.1.2 Micrometeoroid Survivability:

Additionally, these multi-kilometer long wire structures will be exposed to the interplanetary micrometoroid environment, and impacts with these hypervelocity particles will cause cuts to the wires. A preliminary analysis of the probability survival of wire structures, discussed below, indicates that a multi-line structure with multiple redundancies, such as the Hoytether structure, is necessary for missions of any significant duration. For multi-kilometer wires required to provide high survival probability for multi-year durations, this survivability requirement will drive the wire mass more so than the conductivity requirements.

3.2.1.3 Material:

Table 2 compares the characteristics of several candidate conductor materials. These materials all provide sufficiently low resistivity to keep voltage drops along the wire to be less than a percent of the applied bias voltage. Of these materials, Amberstrand (metalized Zylon fiber) provides the highest strength-per weight and more than adequate conductivity. It also has significantly better flexibility than aluminum or copper wire. However, the smallest COTS Amberstrand yarn size (66 filaments) has a larger diameter than desirable for E-Sail applications. It may be possible to acquire a custom Amberstrand yarn that has fewer filaments, albeit likely at higher cost than the COTS configuration. Between the two metal wire options, Aluminum provides better conductivity per mass, but Copper provides superior conductivity per volume. Because the current collected by the biased wires scales with the diameter of the wire, and thus the bias power requirements scale with the diameter. Additionally, Copper is much easier and less expensive to draw to very fine diameters, and fine Copper wires are significantly more robust than fine Aluminum wires.

Table 2. Wire Material Candidates.

	Amberstrand		CNT yarn		Aluminum	Copper
Filament count, or wire size	66	166	1	4	35 ga	35ga
Diameter (µm)	230	370			142	142
Linear mass (g/km)	56	140	10	24	43	142
Each Wire length (km)	5	5	5	5	5	5
Wire mass (g)	280	700	50	120	260	860
Wire Strength (N)	41	105	15.00	36.00	1.96	8.04
Estimated material cost ($/km)	1300	1704	10000	25000	600	800
Est. Packed Volume @ 10 wires (cc)	140	350	125	300	961	961
Resistivity (ohms/m)	9	3	160	70	1.77	1.08

Because the thrust achievable by the ES sail scales proportionately with the tensile strength of the wire, the optimal choice of material appears to be Amberstrand 66, which provides 20X the strength of 35 gauge Aluminum with only 30% higher linear mass.

3.2.1.4 ES Wire Structure Design and Survivability:

Ensuring that the wire structures will have a high probability of surviving the micrometeoroid environment for multi-year durations will require a structure with multiple interconnected lines for redundancy, such as a Hoytether structure[15]. A Hoytether structure is composed of one or more 'primary lines' running the longitudinal length of the structure which are periodically interconnected by 'secondary lines' using knotless connections. The periodic interconnections provide multiple redundant paths to carry loads and currents around strands that suffer cuts due to MM/OD impacts.

Seppänen has demonstrated automated manufacture of kilometer-scale Hoytether structures composed of fine aluminum wires, as illustrated in Figure 12[16].

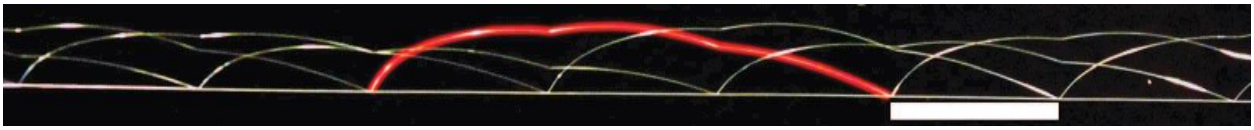

Figure 12. 4-wire system fabricated by Seppänen using 50 µm and 25 µm aluminum wires. White bar is 1 cm long. Red highlighting shows one full secondary loop.

A similar structure can be fabricated in a relatively straightforward manner using an untwisted Amberstrand-66 yarn by periodically bonding a portion of the 66 filaments in the yarn together using ultrasonic welding, soldering, or conductive adhesives, and adjusting the filament lengths in each section to ensure that some of the filaments can spread out from the main bundle under the influence of electrostatic repulsion caused by the ES bias voltage. Alternately, several yarns of Amberstrand could be braided together to form a Hoytether structure using TUI's Torchon Lace braider.

3.2.2 Deployment Model

The system for deploying the E-Sail must be capable of extending a very large (diameters of multiple kilometers), extremely gossamer structure composed of multiple very thin wires. In order to keep the wires oriented perpendicular to the solar wind direction, it is necessary to set the system into rotation so as to provide centrifugal forces to tension the wire structures in order to counter the solar wind force that will tend to blow the wires 'behind' the spacecraft. Figure 13 illustrates the notional basic configuration concept for the E-Sail.

3.2.2.1 Basic Deployment Conops:

This basic concept configuration, however, presents two significant technical challenges. To ensure the wires stay aligned mostly perpendicular to the solar wind (rather than being blown behind the spacecraft), the centrifugal tension on the wire should be roughly a factor of five times the solar wind force. This requires a spin rate on the order of once per hour, which, while slow, requires that the system provide a very large amount of angular momentum to the E-Sail structure. For a multi-kilometer wire length, a simple deployment scheme where the spacecraft is first spun up and then the wires allowed to unspool outward under centrifugal force is not viable because the initial spin rate required to provide the necessary final spin rate once the wires are deployed would be many millions of revs per second.

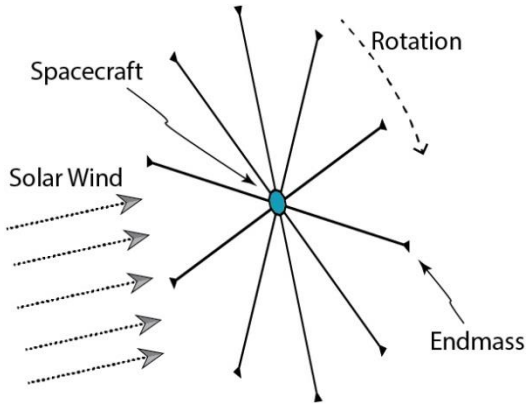

Figure 13. Notional E-Sail concept configuration.

Second, because the forces on the individual wires are likely to vary depending upon orientation to the solar wind as well as due to local variations in solar wind speed, density, and direction, their rotation rates around the central spacecraft will vary, and so it is necessary to provide a means to ensure the lines remain separated and do not collide or tangle. Janhunen's original concept proposed the use of continuous controlled variation of each wire's length to maintain constant rotation rates. However, this method introduces significant system complexity and would require the wires to be continually reeled in and out, which may be problematic for a multi-line wire that will experience multiple cuts to its individual lines during its lifetime.

To simplify the concept, Janhunen proposed connecting the ends of each wire line to its two adjacent lines using non-conducting 'auxiliary wires' strung around the circumference, as illustrated in Figure 14[15]. At the end of each of the primary wires, a "Remote Unit" sub-satellite would be used to deploy both the main wire and the auxiliary wires. Thrusters on these remote units could accomplish the spin-up of the E-Sail system. While technically feasible, this approach presents several drawbacks. First, deployment and spin-up of the system would require tightly coordinated thrust operations of the multiple Remote Unit as well as coordinated operation of all of the multiple wire deployers on the Remote Units. Additionally, the mass of these multiple Remote Units, each with three wire deployers and multiple thrusters will reduce the thrust-to-mass performance of the E-Sail system. Figure 15 shows Janhunen's proposed system configuration for stacking 50 trapezoid-shaped 'remote unit' subsatellites to accomplish

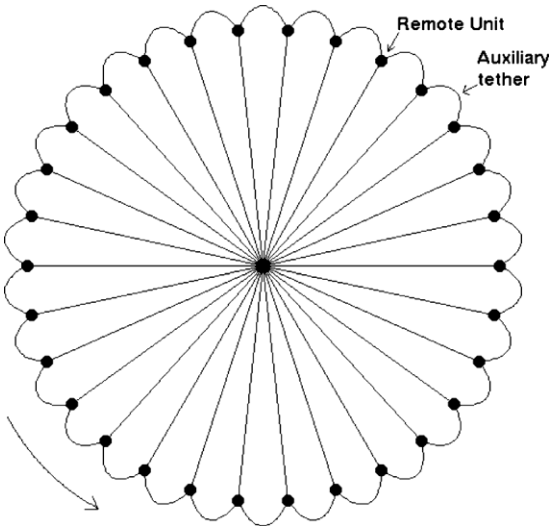

Figure 14. E-Sail with auxiliary wires to maintain separation between radial wires.

deployment of the main and auxiliary wires[17]. Each remote unit would also integrate a cold gas thruster to enable spin-up and control of the system, as illustrated in Figure 16.

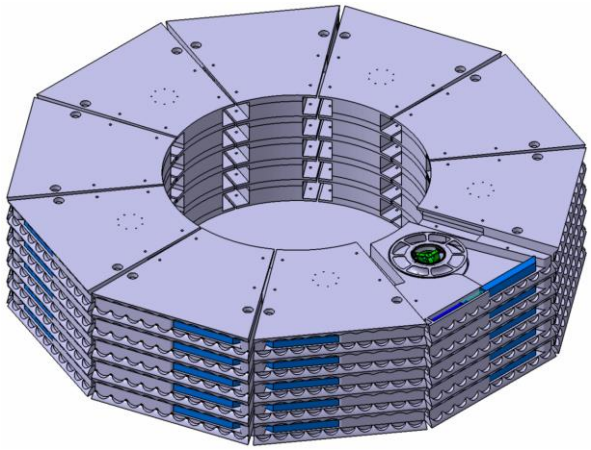

Figure 15. Janhunen ES-sail system concept, with 50 'Remote Unit" subsatellites for deploying main and auxiliary wires and spinning up the system.

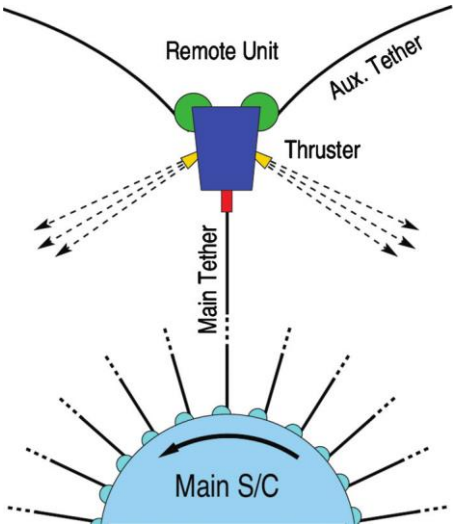

Figure 16. Wire endmass control unit proposed by Janhunen.

While Janhunen's concept is technically feasible, it has high complexity, requiring successful, coordinated operation of a very large number of mechanisms to achieve deployment and spin-up of the E-Sail system. It also results in the system requiring a large total mass of hardware, which will limit its thrust performance. Consequently, in this work we suggest an alternative deployment scheme intended to minimize the system complexity.

3.2.2.2 "Chinese Fan" Deployment CONOPS:

Here we propose a new deployment CONOPS that can potentially significantly reduce the complexity and mass of the hardware required to deploy and spin-up the E-Sail structure. In this concept, the E-Sail wire configuration is similar to Janhunen's 'flower-petal' concept, except that one pair of adjacent primary wires are not connected by an auxiliary wire, so that it has a structure similar to a Chinese Fan, as illustrated on the left in Figure 17. Instead, a 'Crawler' mechanism is initially positioned at the spacecraft end of those two wires. The E-Sail structure can then be folded by pulling the center of each auxiliary wire in the direction perpendicular to the E-Sail's plane, resulting in a linear bundle of wires as illustrated on the right in Figure 17. This bundle of wires and auxiliary wires can then be wound on a spool in a single deployer. Figure 18 illustrates how then the E-Sail structure would then be deployed by a single sub-satellite, with thrusters on either the deployer subsatellite or the main spacecraft ensuring the wires remain taut as the structure is deployed.

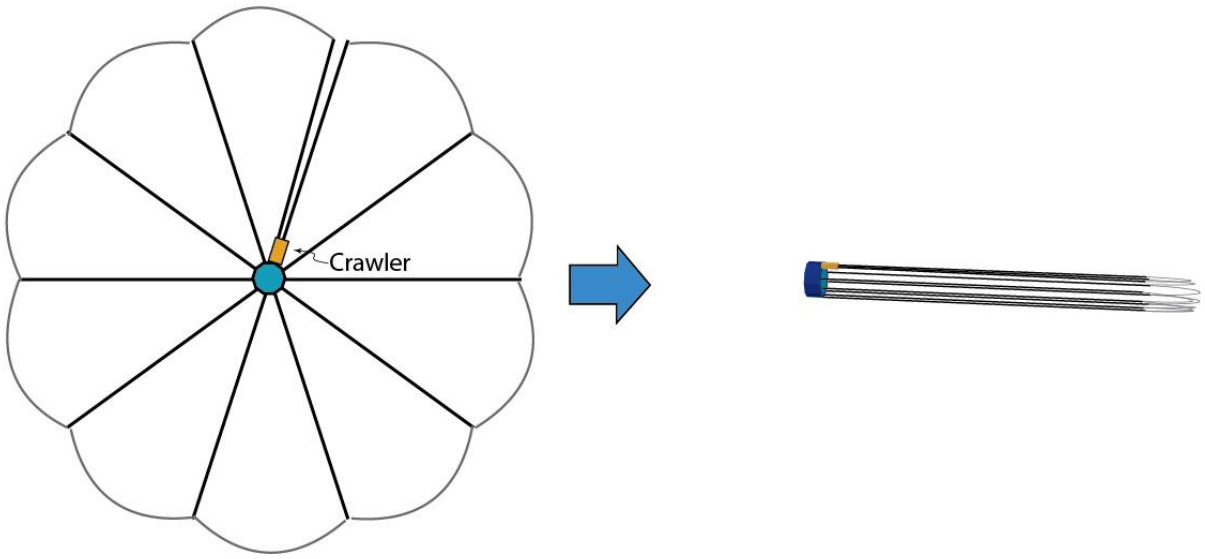

Figure 17. Concept for stowage of the E-Sail structure as a single bundle of wires.

Figure 18. Concept for deployment of the E-Sail structure from a single deployer.

Once the full length of the wires is deployed, the deployer sub-satellite would thrust perpendicular to the wire orientation so as to set the system in rotation, as illustrated in Figure 19

Figure 19. Concept for spin-up of the E-Sail structure with a single sub-satellite.

Once the system reaches the desired rotation rate, the deployer would release all of the auxiliary lines except for one at the edge of the 'Chinese Fan' structure, and the sub-satellite would continue to thrust (at low thrust levels) so as to spread out the fan into a full circle, as illustrated in Figure 20. The primary vehicle would likely need to perform some thrusting and attitude control to ensure it does not become tangled in the wire lines. Having completed its duties, the deployer sub-satellite could then release from the E-Sail wires so that its mass does not impact the E-Sail performance. To complete the structure, the 'Crawler' vehicle would then slide out along the two edge wire lines, under the force of centrifugal acceleration and, if necessary, assisted by simple pinch roller mechanisms, as illustrated in Figure 21, constraining the two edge wires together and completing the circular E-Sail structure.

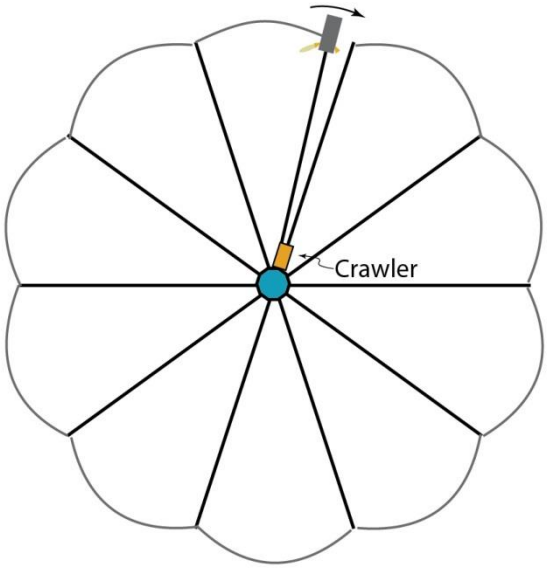

Figure 20. Concept for spreading the radial lines apart.

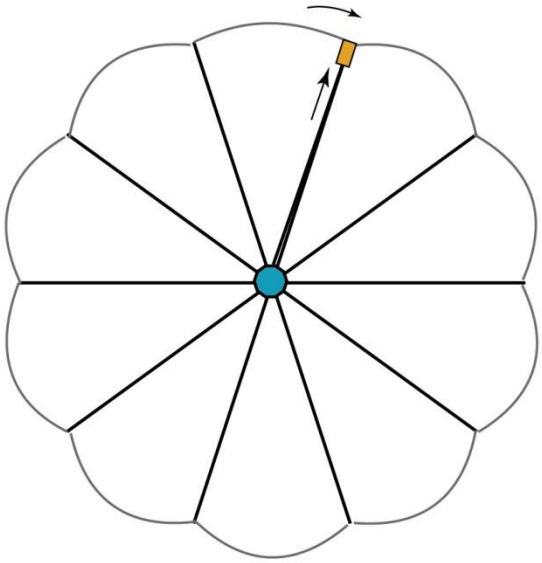

Figure 21. The crawler system would then crawl/slide out along the two edge wires to 'sew' the structure into a circle.

Advantages of this deployment approach are that the multi-wire structure can be assembled in a straightforward manner as the wires are wound onto the deployer spool, and the number of radial wires can readily be increased without requiring additional deployer hardware.

The hardware necessary to deploy this E-Sail structure all has high technical maturity. Figure 22 shows a 1.5U scale wire deployer that TUI developed for the MAST CubeSat experiment. In this deployer, the wire is wound around a spool with 1 twist per turn, so that it can then be pulled off of the end of the spool with no net twist imparted. This type of deployer can be scaled readily. Based upon prior experience, we estimate that a deployer sized to hold a structure with 50, 10-km long Amberstrand-66 wires and the required auxiliary wires will have a diameter of approximately 40 cm and a height of approximately 70 cm.

Figure 22. Wire deployer developed for the MAST CubeSat experiment.

Figure 23 shows a wire crawler CubeSat developed and flight qualified for the MAST experiment, along with the simple pinch-roller mechanism the CubeSat uses to crawl along the wire. This mechanism would be suitable for use in 'sewing' the edges of the chinese-fan E-Sail together to achieve a circularly symmetric structure.

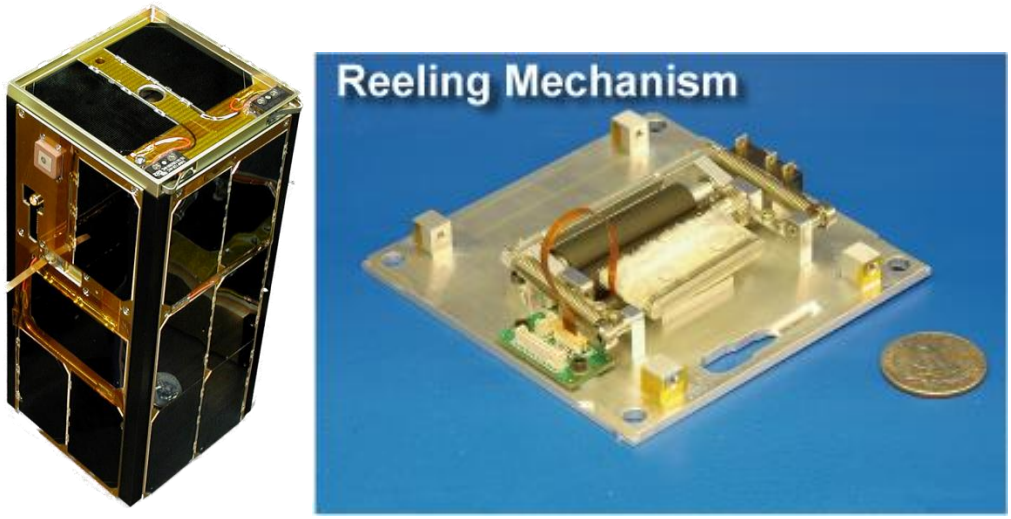

Figure 23. Wire crawler CubeSat and the pinch-roller reeling mechanism developed for the MAST experiment.

3.2.2.3 "Momentum Wheel" Deployment CONOPS:

The momentum deployment method uses existing Control Moment Gyroscope (CMG) hardware with the wires installed on one wheel and the other wheel has a combination spin up motor/generator (**Error! Reference source not found.**). The heels are initially spun up to manageable levels and then the wires are partially deployed. Once the wires are deployed a short distance (0.5 to 1 km) the system begins to manage the angular momentum by alternatively slowing adding angular momentum to the wires and then removing momentum from the second wheel by producing electrical power. The process must be carefully managed in order that the angular momentum added does not accelerate the wheels without accelerating the wires and maintain the centrifugal acceleration on each wire. The idea is to keep the second wheel from being accelerated to very high rotations

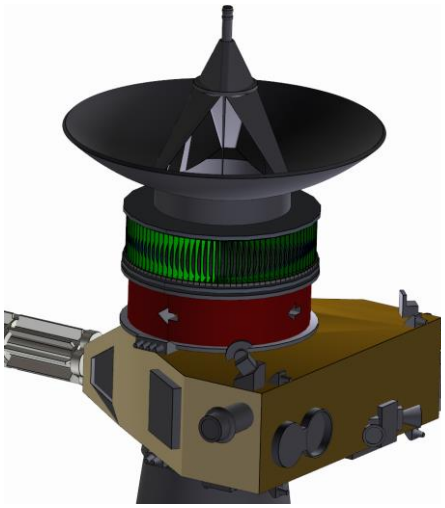

Figure 24: Momentum managed deployment concept

Section 4: Scientific Package

The interaction of the heliosphere with the local interstellar medium (LISM) results in a complicated series of boundary regions. The Voyager 1 and 2 spacecraft are exploring these distant boundaries in situ, as is the Interstellar Boundary Explorer (IBEX) from 1

AU, which measures energetic neutral atoms created in the distant reaches of the heliosphere and LISM. Voyager 1 has crossed the Heliopause and is beginning to explore interstellar space. The next step in the exploration of the Heliopause and interstellar medium is the construction of a fast robotic spacecraft capable of reaching the heliospheric boundaries and beyond on a 25 year spacecraft lifetime. The instrument packages listed here refer to HERTS.

The attached documents provide a master list of desirable instruments for the E-sail mission. Each instrument is culled from a description in the literature, particularly Interstellar Heliopause Probe (IHP) and Innovative Interstellar Explorer (IIE). Interstellar Probe is not directly referenced since the ISP

instrument package is consistent with the instrument choices made here, but the ISP team did not provide a detailed listing of mass, power and data requirements. The master list may be regarded as a comparison and synthesis of the proposed IHP and IIE missions.

Other possible instrumentation that is not discussed but which may be of interest in a mission includes a "star tracker" of some form to ensure that the attitude is known precisely at all times. This should perhaps be part of the payload list provided here. We note that too that there is (a) a concern in how the 10 km wires of the e-sail influence some of the measurement capabilities, and (b) an opportunity in whether the tethers can be used as sensors of the plasma environment. This aspect will need to be addressed eventually by the HERTS team.

Finally, a deluxe payload would contain additionally: a Kuiper Belt Object (KBO) imager/imaging telescope; a detector for molecules; and perhaps a sensor capable of detecting CR anti-protons. These are not discussed for the present since, while they are interesting additional instrumentation opportunities, they are not fundamental to the basic scientific objectives of a mission such as HERTS.

Desired List (subaward sow) :

1) Sensor purpose,
2) Sensor Name,
3) Manufacturer or Supplier of Sensor,
4) Mass of Sensor,
5) Date Rate of Sensor,
6) Power Requirements (Peak & Average) of Sensor,
7) Type of Data Interface of Sensor,
8) Required Size of Sensor (Volume),
9) Estimated Duty Cycle of Sensor,
10) Sensor Pointing Requirements,
11) Other Sensor Requirements (as needed, such as Stability Requirements, Thermal conditioning requirements, etc.)

4.1 HERTS Strawperson Scientifict Payload

This section provides a full listing of possible instruments

4.1.1 Fields

MAG – magnetic field
Purpose: measures the three components of the magnetic field
Mass: 1.5 kg (IHP); 8.81 kg (IIE) because of inclusion of a mast
Data rate: 50 bps (IHP); 130 bps (IIE)
Power: 1.0 W (IHP); 5.30 W (IIE)
Volume: 500 cc (IHP)
Special requirements: magnetically clean spacecraft; assess access of pristine solar wind to an instrument boom.

IHP particulars: 1 Hz sampling;
IIE particulars: 2-three-axis fluxgate magnetometers; do one sample per day from each magnetometer (onboard processing from multiple samples per spacecraft roll period). IIE implementation: 65 bits/sample x number of samples per day x number of sensors; inboard and outbor fluxgate

magnetometers mounted on 5.1 m, self-deployed AstroMast 1324; sensors 184g each and electronics box.

PWS – plasma wave sensor
Purpose: measures the electric field power spectra
Mass: 5.8 kg (IHP); 10 kg (IIE)
Data rate: 30 bps (IHP); 65 bps (IIE)
Power: 2.80 W (IHP); 1.60 W (IIE)
Volume: 19 x 18 x 2 cc (IHP)
Special requirements: magnetically clean spacecraft; assess access of pristine solar wind to an instrument boom.

IHP particulars: Radio and plasma waves from 10 Hz to 10 MHz.
IIE particulars: Three 20-m self-supported antennas; measure E-field vectors up to 5 kHz; no search coils (no B-field components). Implementation: From Voyage: 115,000 kbps → 12.5 kilosamples per second with a 14 bit A/D. Collect 2048 samples and do onboard FFT-frequency of processing limited by onboard available power. Then wait to do next sample. Special requirements: Antenna at least ~20m length.

4.1.2 Plasma Particles

PLS – interstellar and solar wind plasma
Purpose: ion and electron pitch angle distribution functions; composition
Mass: 1.5 kg (IHP); 2.0 kg (IIE)
Data rate: 30 bps (IHP); 10 bps (IIE)
Power: 1.20 W (IHP); 2.30 W (IIE)
Volume: 25 x 25 x 25 cc (IHP)
Special requirements: none

IHP particulars: Ions 0.02-20 keV/q
IIE particulars (two sensors): Plasma ions and electrons from the solar wind, interstellar wind, and interaction region; thermal, suprathermal, and pickup component properties and composition. Mount perpendicular to spin axisl need clear FOV for a wedge 360^{o} around by ~±30°. IIE special requirements: Clear FOV in direction to Sun, clear FOV in direction anti-Sun; equipotential spacecraft.

EPLS – Extended interstellar and solar wind plasma
Purpose: extended-energy ion and electron pitch angle distribution functions; composition
Mass: 2.0 kg (IHP); 1.5 kg (IIE)
Data rate: 30 bps (IHP); 10 bps (IIE)
Power: 1.30 W (IHP); 2.50 W (IIE)
Volume: 25 x 25 x 25 cc (IHP)
Special requirements: none

IHP particulars: Ions 0.2-50 keV/q
IIE particulars: TOF plus energy measurements give composition and energy spectra; ~20 keV/nuc to ~5 MeV total energy for ions in 6 pixels; electrons ~25 keV to ~800 keV. Mount perpendicular to

spacecraft spin axis; clear FOV of 160° x 12° wedge; on-board processing with magnetometer output to get pitch-angle distributions for downlink.

4.1.3 Energetic Charged Particles

CRS – cosmic ray spectrometer
Purpose: ACR, GCR: differential flux spectra by composition; dE-E and range
Mass: 3.5 kg (IHP); 3.5 kg (IIE)
Data rate: 15 bps (IHP); 5.0 bps (IIE)
Power: 4.0 W (IHP); 2.50 W (IIE)
Volume: 15 x 20 x 25 cc
Special requirements: none

IHP particulars: Electrons: 1-15 MeV; H and He: 3 – 300 MeV/n; O-Fe: 5 – 300 MeV/n
IIE particulars: Energy Range on ACR end (stopping particles): H, He: 1 to 15 MeV/nuc; Oxygen: ~2 to 130 MeV/nuc; Fe: ~2 to 260 MeV/nuc. Energy Range on GCR end; Electrons: ~0.5 to ~15 MeV; P, He: 10 to 100 MeV/nuc stopping 100 – 500 MeV/nuc penetrating; Oxygen. Implementation: Measure ACRs and GCR with 1>!Z>!30: double-ended telescope with one end optimized for ACRs and the other for GCRs. It would also measure penetrating particles as is done on Voyager so that both ends need to have clear FOVs. GCR end FOV 35°; clear FOV.

LiCRS (IHP: ELZI) – low-Z energetic charged particles
Purpose: low-Z ions, electrons, positrons, high-energy; method: Si detector, dE/E. Yields differential flux spectra
Mass: 3.0 kg (IHP); 2.30 kg (IIE)
Data rate: 10 bps (IHP); 3.0 bps (IIE)
Power: 3.0 W (IHP); 2.0 W (IIE)
Volume: 10 x 10 x 15 cc
Special requirements: none

IHP particulars: Electrons: 50 keV-2 MeV; H and He: 0.1-10 MeV/n
IIE particulars: Energy Range: positrons: 0.1 to 3 MeV; electrons: 0.1 to 30 MeV; gamma-rays: 0.1 to 5 MeV; H: 4 to 130 MeV/nuc; He: 4 to 260 MeV/nuc; FOV = 46° full cone; Geometry Factor = 2.5 cm2sr. Measurement technique: dE/E (e-, H, He); annihilation (e+)

IHP only: **STI – Suprathermal ion spectrometer**
Purpose: low-Z ions, electrons, positrons, high-energy
Mass: 3.0 kg (IHP);
Data rate: 10 bps (IHP);
Power: 3.0 W (IHP);
Volume: 15 x 15 x 20 cc (IHP)
Special requirements: none

IHP particulars: elements He-Fe, 5 keV – 5 MeV/n; method: ESA, TOF, dE/E

4.1.4 Dust Particles

Dust

Purpose: Dust counter like student dust counter (SDC) on New Horizons
Mass: 1.1 kg (IHP); 1.75 kg (IIE)
Data rate: 20 bps (IHP); 0.05 bps (IIE)
Power: 1.0 W (IHP); 5.0 W (IIE)
Volume: 24 x 24 x 29 cc (IHP)
Special requirements: none

IHP particulars: see Cassini, TOF; speed, mass, composition
IIE particulars: same as student dust counter on New Horizons.

4.1.5 Neutral Particles

Neut – low-energy Neutral Atoms
Purpose: single pixel neutral flux from ram direction
Mass: 2.5 kg (IIE)
Data rate: 1.0 bps (IIE)
Power: 4.0 W (IIE)
Special requirements: none

IIE particulars: Measure neutral H and O at >10 EV/nucleon incoming from interstellar medium (10 eV/nuc ~44 km/s; incoming neutrals are at ~25 km/s with respect to the Sun]. Single pixel; mount looking into ram direction; conversionplate technology. Clear FOV in anti-Sun (ram) direction. Yields neutral distribution functions.

ENA – Energetic Neutral Atoms
Purpose: flux of energetic neutral atoms
Mass: 4.5 kg (IHP); 2.50 kg (IIE)
Data rate: 20 bps (IHP); 1.0 bps (IIE)
Power: 6.0 W (IHP); 4.0 W (IIE)
Volume: 60 x 60 x 50 cc
Special requirements: none

IHP particulars: Hydrogen ENAs 0.05-4 keV. Nine sensors, fan, 20x20deg2 each. Conversion surface, MCP, TOF; and a direct impact sensor for low-UV environments.
IIE particulars: Energy Range: View 0.2 to 10 keV neutral atoms, 1 pixel; ~6° x 6° FOV, mount with sensor looking perpendicular to spacecraft spin axis. 1-axis scanner perpendicular to spin axis.

4.1.6 Neutral Particles

Lyalph – Lyman-alpha backscatter experiment
Purpose: H Lyman-alpha flux
Mass: 0.3 kg (IIE)
Data rate: 1.0 bps (IIE)
Power: 0.20 W (IIE)
Special requirements: none

IIE particulars: Single-channel/single-pixel photometer (at 121.6 nm) similar to those on Pioneer 10/11 (but without the 58.4 mm channel). Implementation: Mount perpendicular to nominal spin axis; need clear FOV (~4° x 4°). 1-axis scanner perpendicular to spin axis.

Alternative: (IHP)
Lyalph – Lyman-alpha backscatter experiment
Purpose: backscattered H Lyman-alpha flux
Mass: 1.20 kg (IHP);
Data rate: 50 bps (IHP);
Power: 1.5 W (IHP);
very low duty cycle

Ly-α broadband photometry.

Section 5: Mission Design

E-Sail technology is a high performance propulsion system that allows demanding missions that are not feasible with other propulsion technologies. However the E-Sail cannot point in an arbitrary direction and as seen in the previous section does present some control issues. Since the direction the force can be pointed in is restricted, the best mission fit for this technology is one that does not require multiple pointing angles.

The Design Reference Mission (DRM) for the E-Sail is the Heliopause mission. The primary goal of this mission is to reach the Heliopause (considered to be the boundary of the solar system at ~ 200 AU) as soon as possible. This mission requires the E-Sail to be at the same angle for the most of the mission, and when it does change, it changes slowly. Since the E-Sail has constraints on the ability to point and maneuver the sail, the Heliopause mission is well-suited to E-Sail technology.

A figure of merit for the performance of an E-Sail is characteristic acceleration, a parameter borrowed from solar sails. The characteristic acceleration is defined as the acceleration achieved when the E-Sail spacecraft is pointed directly at the Sun (i.e., the sail plane is normal to the Sun vector) at 1 AU. Characteristic acceleration values for preliminary designs of E-Sails have been published by Janhunnen in several references. Quarta and Mengali [ref] build on his work and present mission design results for a range of characteristic accelerations from 0 to 2 mm/sec^2 where 2 mm/sec^2 is considered the upper end of the performance range based on previous work by Janhunnen. By contrast, 0.5 mm/sec^2 is considered a high level of performance for a solar sail. For the purposes of this mission design study, we chose 1 mm/sec^2 and 2 mm/sec^2 as “nominal” and “high performance” E-sail characteristic accelerations.

Section 6: Vehicle Control

The initial study of the deployed wires indicates that applying a biased voltage to each side of the system will provide for thrust vector control (TVC). Analysis by Janhunen predicts that vectors up to 30 degrees off the solar wind direction are possible. This prediction was included with the ground rules and assumptions for the Phase I effort but must be verified with simulation for Phase II.

A method to steer the thrust vector generated by the wires is required for vehicle navigation. The net force generated by the charged wires will act through an effective "center of pressure" (CP). That CP will be at some offset from the vehicle center of mass (CM). Having a method of controlling the CP/CM offset distance is crucial to steering the thrust vector for putting the spacecraft on the desired trajectory. The CP/CM offset will also be useful in the attitude control system (ACS) of the spacecraft. Considering that the spacecraft will be spinning, the TVC and ACS may be complicated by gyroscopic effects. Phase I study has indicated that "turning on or off" or "throttling" the individual wires may provide the required TVC. CP/CM offset control might be supplemented by reaction wheels or by the propulsion system used to spin up the spacecraft.

An investigation into attitude dynamics is required for Phase II. The analytical models will be developed to steer the thrust vector and maintain attitude control, taking into account the deployed wire dynamics. The thrust models and wire dynamics will be simplified in Matlab and combined with the trajectories tools that provide for the gravitational effects and inter-solar system motions. These analytical models will be used to develop a method to steer the thrust vector which would include specifications on the required voltage bias and timing for each of the wires within the system. This can then be integrated into a simulation to serve as an analytical proof-of-concept. The structure of these models exists but must be modified and will depend on the products produced in the PIC simulations and the wire dynamics and control simulations.

The final task to be performed under the Phase II effort will use the products produced to define a development path and establish what additional testing, analytical studies and so on tha must be performed to allow a small scale demonstration to be conducted. The small scale demonstrations will be based on what is needed to be validated for the HERTS scale mission so that the development program does not get off track and focused on small scale projects like cubesats. However a cubesat propulsion systems for deep space is expected to be one of the derivative products produced in these studies.

Section 7: Comparison to Alternative Propulsion Systems

A comparison of propulsion concepts was taken from the Interstellar Probe study performed by the ACO for the Keck Institute for Space Studies (KISS) in which many team members participated. This study compared known or near term low-thrust advanced propulsion system candidates while determining which SLS configuration could deliver the appropriate characteristic energy (C_3) to the spacecraft based on several trajectory options. The candidate propulsion systems included a Magnetically Shielded Miniature (MaSMi) Hall thruster (Figure 25), Solar Sail (Figure 26) and E-Sail (Figure 27). Several possible trajectories were studied involving both single- and multiple-planetary flyby maneuvers to understand if any additional "free" energy could be obtained to boost the speed of the spacecraft toward interstellar space. The systems compared did not exactly match the system studied in the Phase I effort but it was an apples-to-apples comparison of thruster concepts.

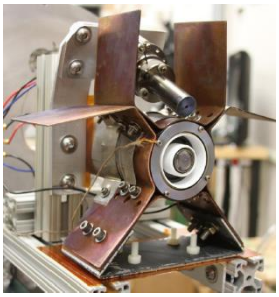

Figure 25: MaSMi Hall thruster system

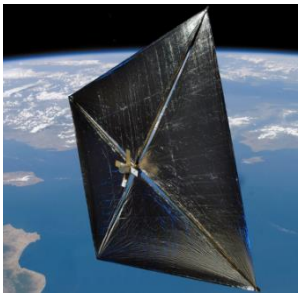

Figure 26: NanoSail-D solar sail system.

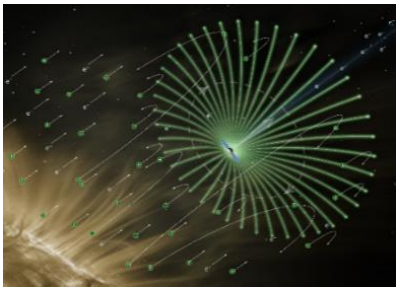

Figure 27: E-Sail system.

7.1 Launch Configurations

The initial study investigated three potential mission profiles targeting a 250 AU spacecraft delivery point based on the aforementioned launch vehicle architecture selection:

(1) a direct escape trajectory per SLS Block 1B C3 performance capability,
(2) an escape trajectory using a powered or unpowered Jupiter Gravity Assist (JGA), and
(3) an escape trajectory using powered or unpowered Saturn-Uranus gravity assists. Lastly, the spacecraft mass was adjusted to determine how much it might impact the overall mission timeline.

The first mission profile employed no additional velocity (ΔV) gains except that which could be imparted strictly by the SLS Block 1B architecture with a 5.0 m (16.4 ft) payload fairing (PLF) (Figure 28). The mission profile was an Earth escape trajectory directly to an orbit with aphelion of 250 AU, neglecting the goal of reaching that distance in 30 years.

Figure 28: SLS Block 1B with EUS and 5.0 m PLF (adapted).

The required heliocentric velocity at earth departure of 42.0 km/s (137,800 ft/s) translates to a C_3 energy of about 150 km^2/s^2, approximately 40 km^2/s^2 greater than the upper bound of the projected SLS Block 1B C_3 capability for the assumed spacecraft mass. Therefore, the spacecraft would not be able to even reach 250 AU without employing either a kick stage and/or gravity assist, let alone be able to reach that distance in 30 years. Using a kick stage at earth departure, however, greatly reduces the total trip time. To estimate the optimal split between kick stage mass and SLS payload capability, various kick stage Propellant Mass Fractions (PMF) were assumed where Fig. 5 shows the relationship between spacecraft velocity after kick stage burnout and SLS C_3 values. A theoretical kick stage with a PMF of 0.90 and specific impulse (I_{sp}) of 450 seconds (approximately equivalent to a common Centaur) could get the spacecraft to 250 AU in about 68 years assuming an SLS C_3 capability of 67.8 km^2/s^2.

The second mission profile incorporated a JGA (Figure 31) and either the same scalable earth departure kick stage as shown above or a SRM. Setting the flyby radius at 350,000 km (217,490 mi) resulted in a trip time of about 49 years to 250 AU for an unpowered flyby. Lowering the flyby distance to 126,000 km (78,296 mi) reduced the time by only a couple of years, still well short of the goal. Adding an additional kick stage for a powered flyby reduces the available mass for the earth departure kick stage and thus departure energy. Figure 30 describes several cases that were analyzed, including 1 km/s, 2 km/s, 3 km/s and 4 km/s. In particular, assuming a SRM kick stage with an I_{sp} of 292 seconds and PMF of 0.90

for the flyby maneuver indicated that a Star 63D motor fit well for a 4 km/s powered flyby. But for this configuration, a Star 63F SRM provided the best performance for an earth departure stage resulting in a total trip time of 40.5 years, while all other cases yielded a longer trip time.

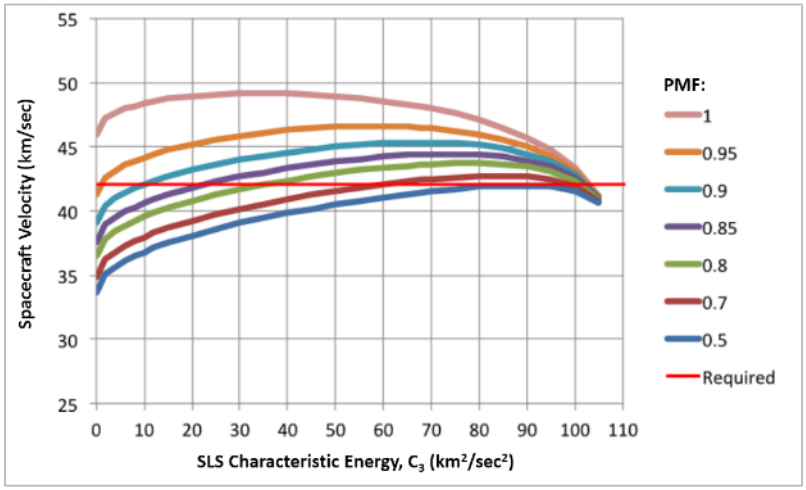

Figure 29: Propellant Mass Fraction (PMF) sweep to size spacecraft kick stage assuming an Isp of 450 seconds.

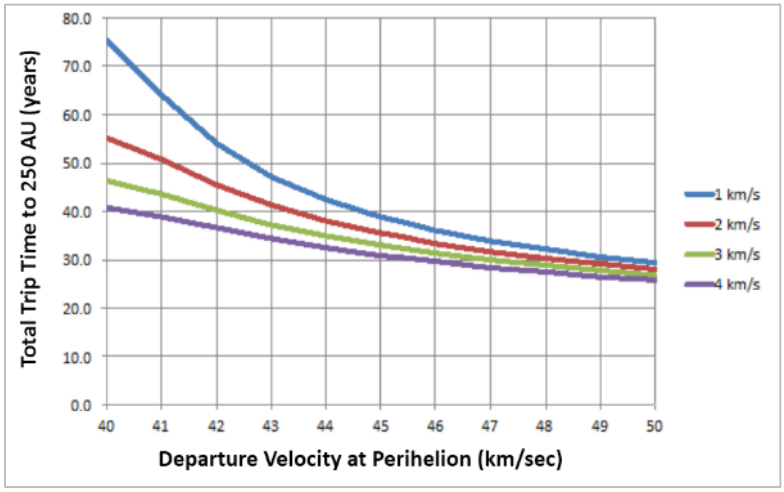

Figure 30: Various trip times to 250 AU for a powered Jupiter Gravity Assist (JGA) trajectory.

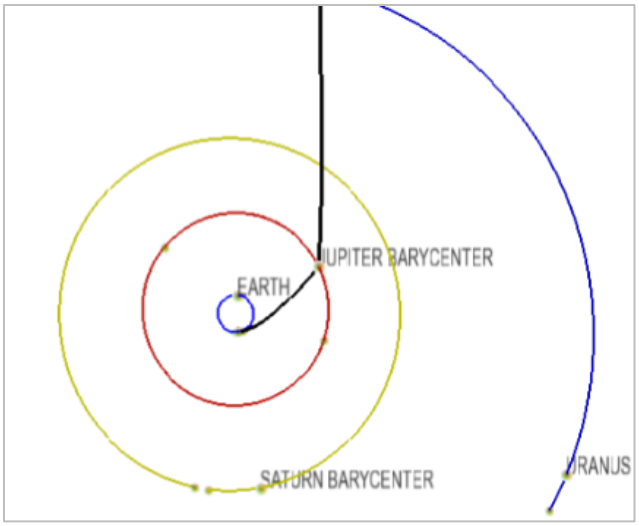

Figure 31: Powered JGA trajectory profile.

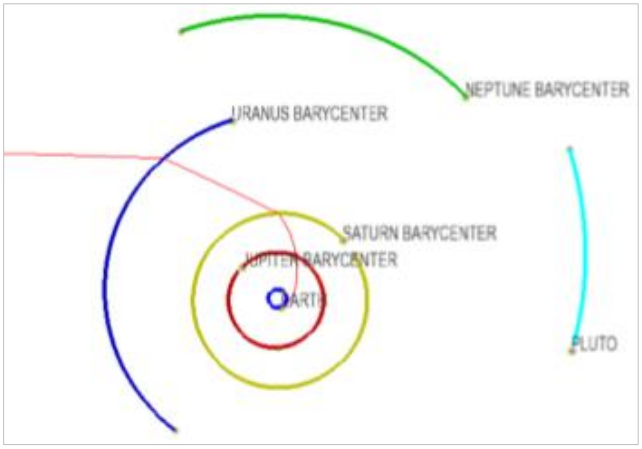

Figure 32: Powered Saturn-Uranus trajectory profile.

The third and final mission profile incorporated a Saturn-Uranus flyby trajectory (Figure 32), including powered assists at both planetary bodies when possible. To compete with the powered Jupiter flyby, each powered assist would need to provide a ΔV of 4 km/s (13,100 ft/s). Unfortunately, after accounting for the additional mass required adding a second kick stage, the entire payload (Interstellar Probe plus two sizeable kick stages) resulted in a mass too heavy for the selected SLS Block 1B architecture. Theoretically, the SLS Block 2B architecture could be assumed but this upgrade will likely not be implemented until much further down the road.

A final analysis was conducted to determine a new total trip time to 250 AU if the mass of the spacecraft and payload attach fitting (PAF) were reduced by half to a combined total of 415 kg (915 lb_m). By doing so it was found that, for the case with a powered JGA of 4 km/s, the total trip time could be reduced by approximately 2-3 years. The Interstellar Probe study discussed subsequently assumed a spacecraft mass close to the 415 kg (915 lb_m), at 380 kg (838 lb_m) in addition to other adjustments to the GR&A. Again, this is different than the HERTS vehicle but it is an apples-to-apples comparison of propulsion concepts.

7.2 Propulsion System Comparison

The GR&A of the KISS Interstellar Probe study were not substantially different from those of the Phase I NIAC study (Table 3). Most importantly, trip times and vehicle mass were comparable.

Table 3: GR&A for current Interstellar Probe study. [18]

Item	Description
Mission Performance	100+ AU in 10 years
Launch Window	2025 – 2035
Launch Vehicle	SLS Block 1B + EUS + 8.4 m PLF
Spacecraft Mass*	380 kg (838 lb_m)
Spacecraft Heat Shield Mass†	300 kg (661 lb_m)
Spacecraft Power	450 W

* Mass includes all components except onboard low-thrust APS.

† Mass scaled from that of Solar Probe Plus heat shield.

Several low-thrust APS technologies were traded for each of the trajectory profiles considered, including a MaSMi Hall thruster, solar sails and an E-Sail propulsion system. In addition to the spacecraft having some kind of onboard low-thrust APS stage, the required quantity and size of aft-attached, series-burn SRM kick stages for various impulsive maneuvers was also assessed. The MaSMi hall thruster, would be powered by the onboard eMMRTG outputting 450 W of power; and, it was assumed, to be capable of 50,000 hours of maximum lifetime and exerting 19 mN (0.004 lb_f) of thrust with an I_{sp} of 1,870 seconds. The solar sail and E-Sail propulsion system GR&A are outlined below in Table 4 and Table 5, respectively.

Table 4: Solar sail propulsion system GR&A.

Item	Description	
Reflectivity	0.91	
Minimum Thickness	2.0 μm	
Maximum Size (per side)	200 m (656 ft)	
Sail Material	CP1	
Aerial Density *	3 g/m^2	10 g/m^2
Characteristic Acceleration	0.426 mm/s^2	0.664 mm/s^2
System Mass	120 kg (265 lb_m)	400 kg (882 lb_m)

** Assumes an advancement in technology. Current technology is approximately 25 g/m^2.*

Table 5: E-Sail propulsion system GR&A.

Item	Description	
System Mass	120 kg (265 lb_m)	
Wire Material (Density)	Aluminum (2,800 kg/m^3)	
Wire Diameter (Gauge)	0.127 mm (36 gauge)	
Characteristic Acceleration	1 mm/s^2	2 mm/s^2
Wire Quantity	10	20
Individual Wire Length	20 km (12.4 mi)	20 km (12.4 mi)

Two trajectory profiles were considered in the study: (1) an escape trajectory using a JGA maneuver (*E-Ju*) and (2) an escape trajectory first performing a JGA maneuver followed by a sun dive via an impulsive Oberth maneuver and Saturn gravity assist maneuver (*E-Ju-Su-Sa*). Both trajectory profiles are depicted in Figure 33 below and are separated based on the type of low-thrust APS employed.

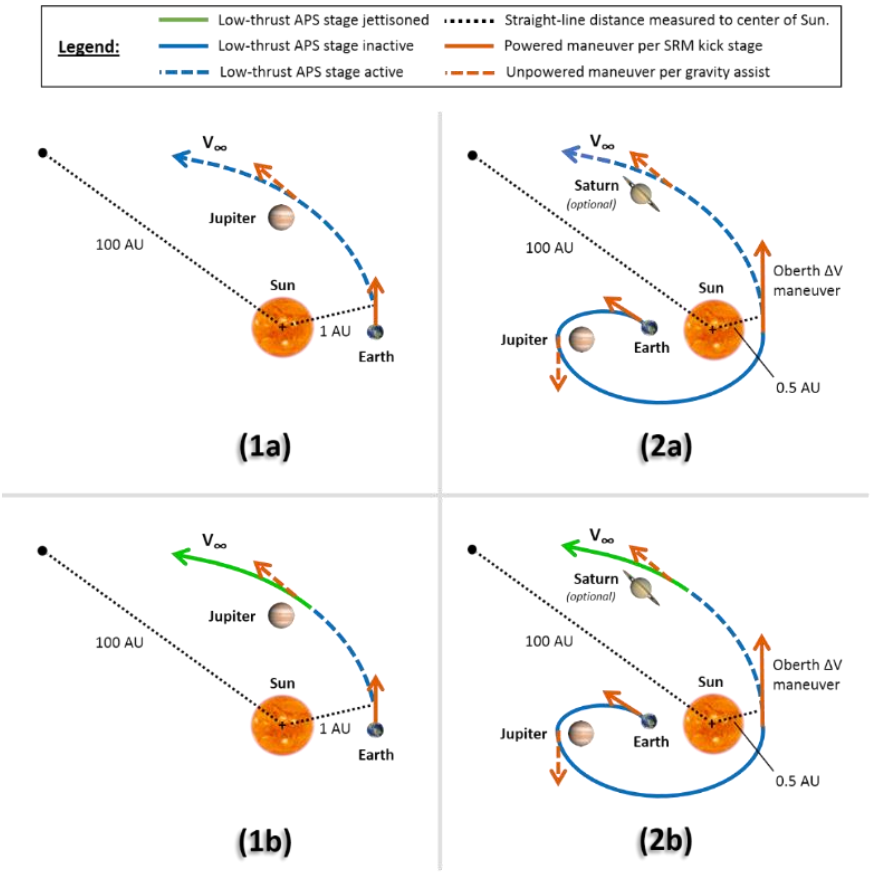

Figure 33: Mission trajectory profile options considered: a) trajectories apply to MaSMi Hall thruster and E-Sail systems and b) trajectories apply to solar sail system.

The first trajectory profile option is similar to the one shown in Figure 31 except for the lower spacecraft mass, shorter target distance and addition of a low-thrust APS stage. The trajectory relies more heavily on the SLS C_3 capability which sets the spacecraft's initial velocity prior to earth departure. At departure, the SLS (with an additional SRM kick stage) delivers the spacecraft on an Earth-escape trajectory. Once outside Earth's sphere of influence, the spacecraft deploys and activates its low-thrust APS. For the MaSMi Hall thruster case, the thruster is operated until the assumed 50,000-hour lifetime is reached. If employing a solar sail, the sail is jettisoned prior to the Jupiter gravity assist. The E-Sail option assumes operation until it reaches a point of diminishing return, estimated to occur at about 20 AU.

As the spacecraft approaches Jupiter, it performs a gravity assist with a minimum flyby distance of 4.89 Jupiter radii. For this analysis, the orbit of Jupiter is assumed to be circular at 5.203 AU. Figure 34 and Figure 35 illustrate the effect of each low-thrust APS type on the total trip time to the termination shock and heliopause at 100 AU. Two E-Sail data points are plotted in Fig. 15 denoted by green square which corresponds to an E-Sail characteristic acceleration of 2 mm/s^2, and a green circle which corresponds to a 1 mm/s^2 characteristic acceleration.

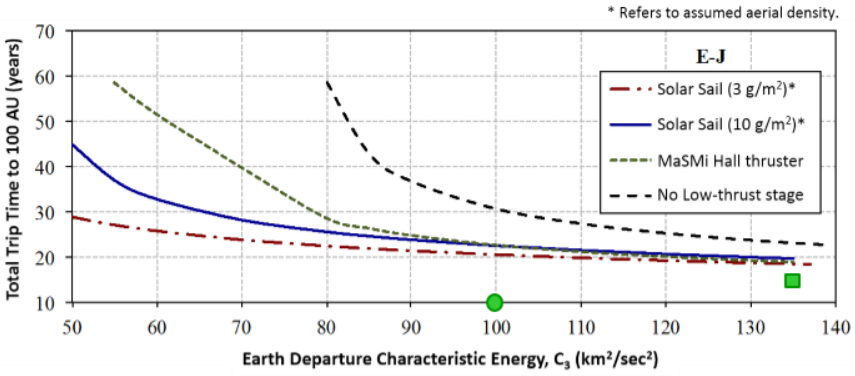

Figure 34: Low-thrust APS analysis for E-Ju trajectory profile.

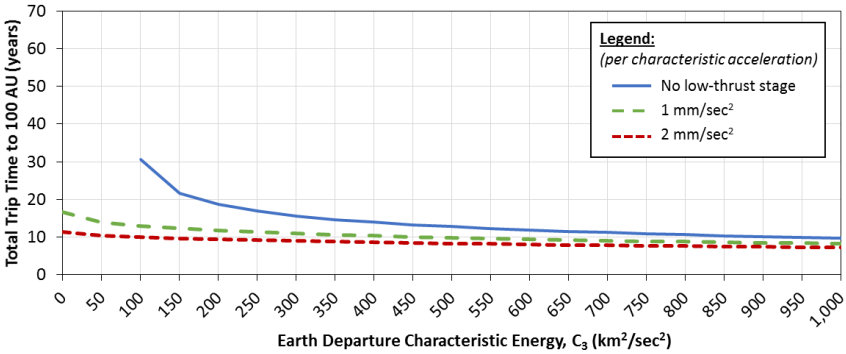

Figure 35: E-Sail propulsion system analysis for E-Ju trajectory profile.

Similar to the first trajectory option, the second trajectory begins with an Earth-departure performed by the SLS and an additional SRM kick stage. With the low-thrust APS yet to be activated, the spacecraft performs a Jupiter flyby, which occurs at a minimum passage distance of 18.72 Jupiter radii, in order to reduce its heliocentric speed such that the resulting perihelion is 11 solar radii (≈0.05 AU). At perihelion, about 2.97 years into the mission, another SRM kick stage performs the final high-thrust maneuver. Approaching this close to the sun requires that the spacecraft's heat shield withstand temperatures upwards of 2,500 °F in addition to "blasts of radiation and energized dust levels" [19] The heat shield, along with the SRM, is jettisoned when the radial distance from the sun is 0.5 AU. This is also where the low-thrust APS is initiated. Similar to the first trajectory option, the MaSMi Hall thruster operates for 50,000 hours, the solar sail is dropped just prior to the next planetary flyby (in this case Saturn), and the E-Sail option is employed until the thrust has a negligible effect. At Saturn, which in this study is assumed to have a circular orbit at 9.583 AU, a final gravity assist is performed with a minimal flyby distance of 2.67 planetary radii. Table 4 describes the SRM kick stages chosen for this particular study for various low-thrust APS masses.

Table 6: SRM kick stages chosen for the E-Ju-Su-Sa trajectory option.

Low-thrust APS Stage Mass	**Impulsive Burn 1 (Earth departure)**	**Impulsive Burn 2 (Perihelion)**	**Notes**
0 kg (0 lb_m)	Star 63D	Star 48V	Star 63D – 20% of propellant offloaded.
120 kg (265 lb_m)	Star 63F	Star 48V	Star 48V – 5% of propellant offloaded.
400 kg (882 lb_m)	Star 63F	Star 48V	Star 48V – 20% of propellant offloaded.

700 kg (1,543 lb_m)	Star 63D	Star 48V	No propellant offloaded for either SRM.

Figure 36 provides additional insight into the target trajectory for option 2 previously shown in Figure 33 above, where the green square corresponds to an E-Sail characteristic acceleration of 1 mm/s^2.

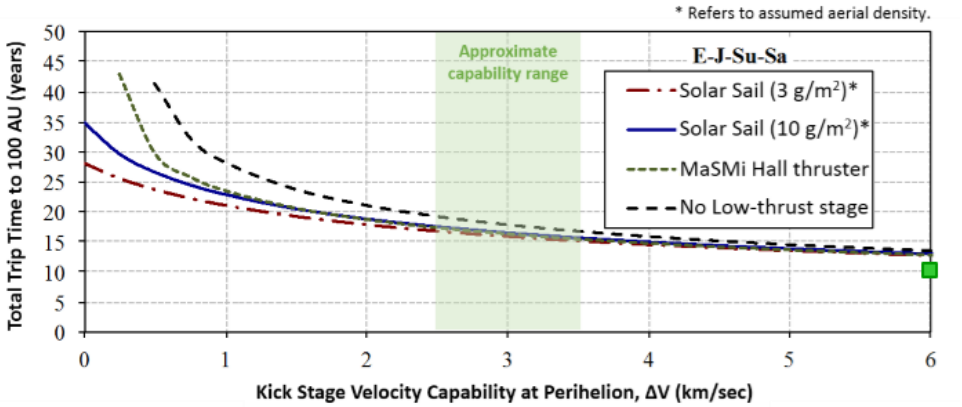

Figure 36. Kick stage analysis for E-Ju-Su-Sa trajectory profile.

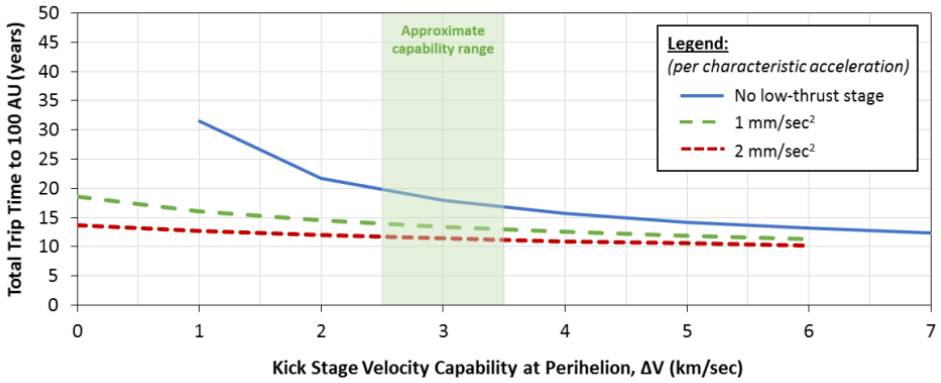

Figure 37. Kick stage analysis for E-Ju-Su-Sa trajectory profile (E-Sail only).

A quick assessment was conducted to determine what the payload might look like inside of a SLS Block 1B 8.4 m PLF (Figure 38). The spacecraft itself was assumed to be volumetrically similar to that of a Voyager 1 or Voyager 2 spacecraft in its stowed configuration. Corresponding to the appropriate low-thrust APS stage mass as shown in Table 4, two SRM kick stages were located below each low-thrust APS stage. The total payload mass was calculated and is quoted above each PLF configuration; it includes the spacecraft bus, low-thrust APS, heat shield and SRM kick stages.

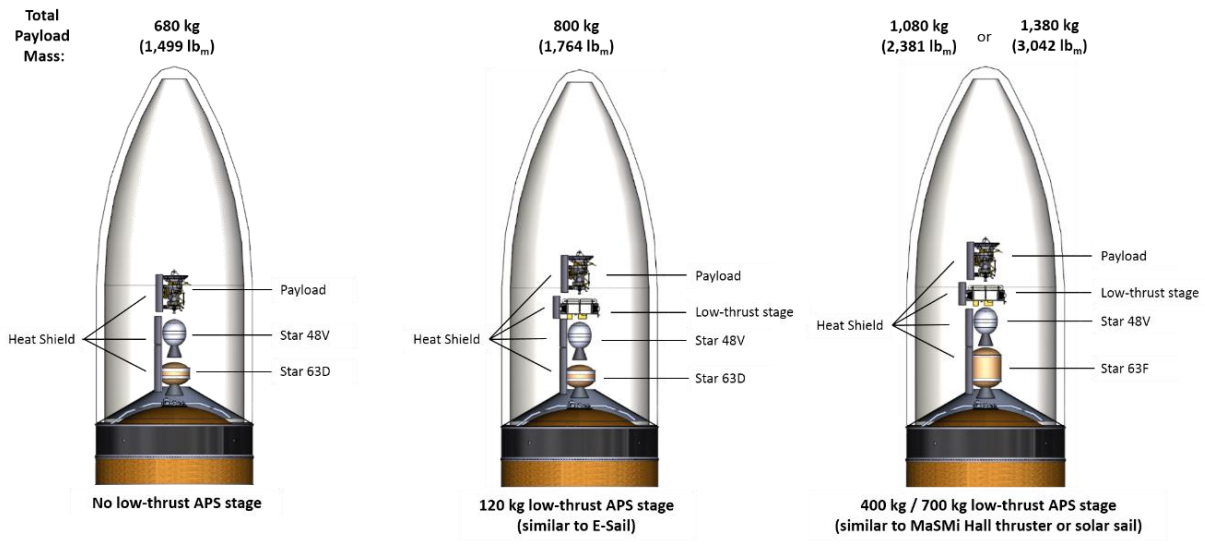

Figure 38. Approximate envelope of payload and SRM kick stages inside SLS 8.4 m PLF per Voyager stow configuration volume.

Figure 39 represents the *E-Ju-Su-Sa* trajectory option in a more detailed fashion in order to show the Jupiter flyby and Oberth maneuvers. The figure itself does not include the optional Saturn flyby, which may or may not be available depending on the launch date. Since adjusting the magnitude, timing and direction of the Oberth maneuver may be necessary for targeting a Saturn flyby, variables such as launch window and energy gain imparted by Saturn could vary significantly as well as total trip time.

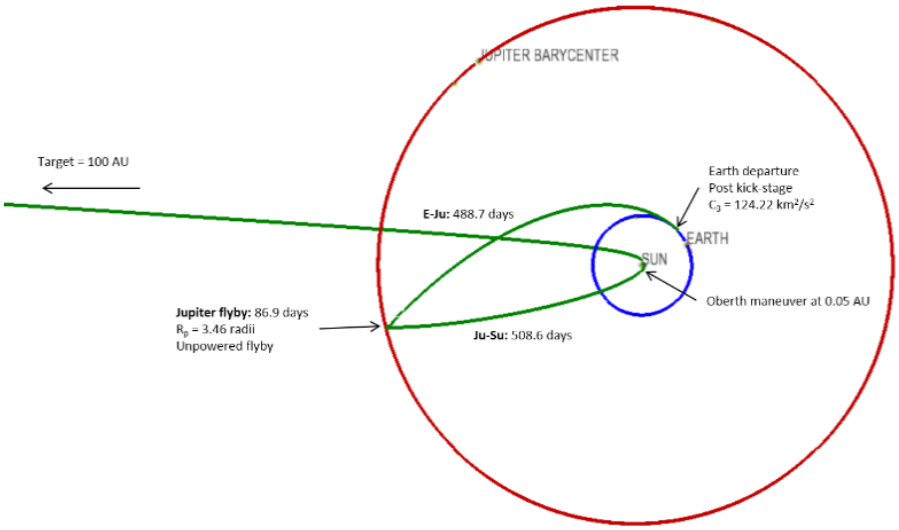

Figure 39. Detailed trajectory for E-Ju-Su-Sa option (Saturn flyby optional).

7.3 Study Results

Conceptual analysis concludes that a spacecraft could reach interstellar space within a noticeably shorter amount of time compared to the VIM when employing low-thrust APS stages. In fact, applying an E-Sail low-thrust APS stage results in the lowest total trip time of approximately 11 years for the *E-Ju-Su-Sa* trajectory option. There is also an additional potential mass, and thus time, savings if a SLS Block 1B 5.0 m PLF is employed rather than the 8.4 m PLF since there appears to be adequate room to do so. With that said, all low-thrust APS technologies for either trajectory option provide substantial total trip time improvements over the VIM ranging anywhere from 11 – 19 years, assuming a maximum applied C_3 capability of 135 km^2/s^2 for an *E-Ju-* trajectory profile or an average perihelion kick stage ΔV of 3 km/s (9,842 ft/s) for the *E-Ju-Su-Sa* trajectory profile. However, for the latter profile, compared to the MaSMi hall thruster and solar sail propulsion systems, having no low-thrust APS stage actually achieves almost the same total trip time especially for perihelion kick stage ΔV's greater than 4 km/s (13,123 ft/s).

It is worth noting that there is one concern specifically for the *E-Ju-Su-Sa* trajectory option and that is the SRM-powered Oberth maneuver performed very close to the sun's surface (11 solar radii or 0.05 AU). Keeping in mind that this is a conceptual study, the assumed heat shield technology is stemming from NASA's Solar Probe Plus mission, which is scheduled to occur before the Interstellar Probe mission. It is uncertain as to how the heat shield would cover the SRM kick stage performing the impulsive perihelion burn while not being simultaneously partially destroyed by the kick stage's plume. In other words, if the heat shield incurs damage then it is a concern as to how the rest of the shield would perform for the duration of the trajectory where the spacecraft is still very close to the sun.

Section 8: Recommended Future Steps towards E-Sails in Space

A review of the observations and findings from earlier sections indicates there are four areas that present significant challenges to the development of the E-Sail propulsion system. These four areas include:

1) Understanding the interaction of the electrons and the sheath
2) Understanding and validating the net thrust on the deployed conductors/wires
3) Deployment of the wires and control of the wires during operational phases
4) Vehicle control when voltages and forces are varying on individual wires.

These four areas represent the most significant risk or challenges to the development program. The remaining subsystems such as the electron emission source / E-Gun, high voltage power supplies and voltage control devices are expected to be derivative of existing hardware. In fact the high voltage power supplies are expected to be very similar in design to those being developed for the next generation electric propulsions systems.

The recommended approach for understanding the interaction of the electrons and resulting sheath/wires is to perform additional chamber testing. Prior testing performed at MSFC in the 1980's provided the enhanced understanding of the electron/proton interaction with charged bodies in space. This provided the team with the data to conclude the actual thrust being proposed originally for the E-Sail was understated. This original testing was performed on relatively large spheres and there is concern on how the small diameter wires will perform.

As discussed earlier PIC modeling is key to understanding how the system will perform in deep space. Testing of long conductors is in-practical on the ground so combining a multistep program where PIC models are verified by the plasma testing and then used to extrapolate to deep space environments. These PIC models will be a key tool to support the design of the E-Sail.

Deployment of the wires was considered a very complex task and while numerous good ideas were examined most was considered too complex to be practical. The team discussed numerous approaches including those presented by our FMI collaborator Dr. Pekka Janhunen. Only two configurations were selected to go forward based on complexity and the ability to provide a mass efficient design. There are several other approaches that remain as second tiers that could be brought forward if neither of the two concepts selected are successful. The two concepts were both simple and minimized new hardware developments. The rocket deployed approach built on TUI experience with long tethers in space. The momentum management approach builds on Control Moment Gyroscopic (CMG) devices that allow a spacecraft to manage the angular momentum with opposing wheels. This is much like power storage concepts developed in the late 90's for energy storage where a pair of opposing wheels would be spun to store electrical power that would be retrieved by reversing the electrical motors and using them as generators. No real ground test can be conducted with long wires to test deployment concepts so high fidelity simulations are required. The use of an existing tether simulation program from TUI called Tether-Sim provides a basis for developing these simulations and assessing the deployment concepts in some detail.

These same simulations will allow the team to assess the wires once fully deployed and operating. The forces on the individual wire including the thrust, and centrifugal acceleration will be assess to ensure there are no unforeseen motions such as skip roping seen on the near-earth tethers systems.

The European studies identified some concerns with vehicle control due to the forces varying from wire to wire. Tacking the vehicle or varying the voltages on individual wires could cause the wires to come in contact with each other. This contact is undesired and must be avoided. Further there are no control laws developed for such a vehicle. These control laws and approaches to managing the wires are a concern to the team. The recommended approach to developing the control strategies and understanding how the vehicle will be steered will require the use of additional simulations. These simulations should build on those performed under the phase I efforts here.

A roadmap for the development of the E-Sail is being to become clear. Obviously the first step is to develop the data and simulations discussed above. These simulations will provide the design data required to develop any scale propulsion system. Clearly a demonstration flight is required to reduce the risk for larger scale programs. Several Cubesat demonstration flight concepts have been developed and should be practical to fly in the 2018 timeframe. These demonstration flights would allow the team to obtain the data and knowledge to retire the most significant risk issues. The figure below provides suggested roadmap to a full scale Heliopause mission that includes a NIAC Phase II effort, a small scale demonstration flight that leads to the full scale flights in the 2025 timeframe.

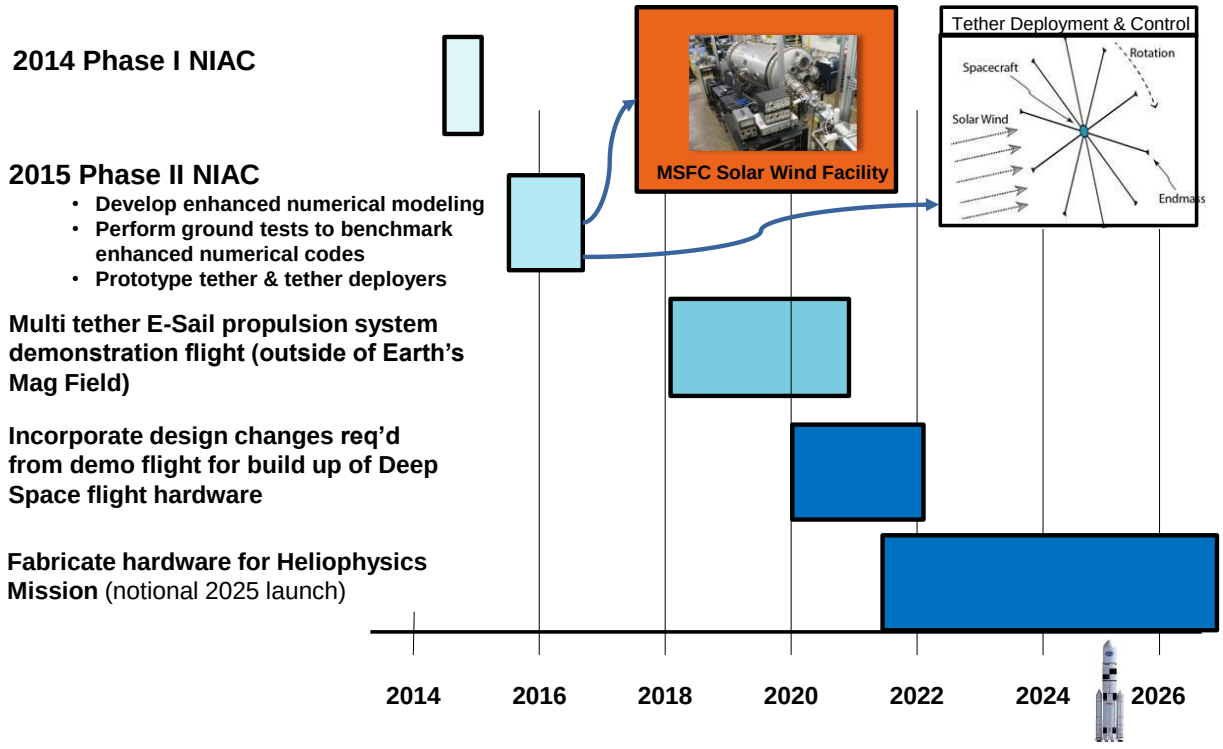

Figure 40: Recommended Development Roadmap for the E-Sail propulsion system.

Section 9: Study Conclusions

The study was very successful in providing the data to determine the transient time to the Heliopause and indicates that travel times of less than a decade are possible. The study identified the most challenging technologies but also identified that all subsystem are derivatives of hardware or concepts that have flown in space before. Cleary the integration of these technologies is very immature at this time but the concept shows excellent potential to provide un-match propulsion into deep space. If the OML theory is proven to be consistent with current characterizations then the E-Sail concept is very scalable from Cubesats to large scale missions to the Heliopause. The propulsion could allow exploration of any of the major planets including both inner and outer planets and their moons. No currently envisioned propulsion system comes close in transient times to deep space objects. The next steps discussed in the previous section should be considered for funding. In addition a small scale demonstrating flight should be considered and early planning started. This early planning would allow the team to use the result of of the proposed studies to incorporate them into a demonstration flight in the 2018 timeframe.

References

(1) Mengali, G., A. Quarta and P. Janhunen, Electric sail perfromance analysis, J. Spacecr. Rockets, 45, 122-129, 2008.

(2) Quarta, A.A. and G. Mengali, Electric sail mission analysis for outer solar system exploration, J. Guid. Contr. Dyn., 33, 740-755, 2010.

(3) Janhunen, P., P. Toivanen, J. Envall, S. Merikallio, G. Montesanti, J. Gonzalez del Amo, U. Kvell, M. Noorma and S. Lätt, Overview of electric solar wind sail applications, Proc. Estonian Acad. Sci., 63, 267-278, 2014.

(4) Mengali, G. and A. Quarta, Non-Keplerian orbits for electric sails, Cel. Mech. Dyn. Astron., 105, 179-195, doi:10.1007/s10569-009-9200-y, 2009.

(5) Quarta, A.A. and G. Mengali, Electric sail missions to potentially hazardous asteroids, Acta Astronaut., 66, 1506-1519, 2010.

(6) http://www.electric-sailing.com/publications.html

(7) Janhunen, P.: Electric Sail for Spacecraft Propulsion, J. Propul. Power, 20(4), 763-764, 2004.

(8) Stone, N. H., The Aerodynamics of Bodies in a Rarefied Ionized Gas With Applications to Spacecraft Environmental Dynamics, NASA Technical Paper 1933, pp 97-102, November 1981.

(9) Janhunen, P., and A. Sandroos, Simulation of solar wind push on a charged wire: basis of solar wind electric sail propulsion, Ann. Geophys., 25, pp

(10) Stone, N. H., B. J. Lewter, W. L. Chisholm, and K. H. Wright, Jr., Instrument for differential ion flux vector measurements on Spacelab 2, Review of Scientific Instruments, 56 No. 10, October 1985.

(11) Langmuir, Irvin and H. M. Mott-Smith, 1924,

(12) Huddlestone, Richard. H. and Stanley L. Leonard (Ed.), Plasma Diagnostic Techniques, Academic Press, New York, pp. 125-131, 1965

(13) Glen H. Fountain, David Y. Kusnierkiewicz, Christopher B. Hersman, Timothy S. Herder, Thomas B Coughlin, William T. Gibson, Deborah A. Clancy, Christopher C. DeBoy, T. Adrian Hill, James D. Kinnison, Douglas S. Mehoke, Geffrey K. Ottman, Gabe D. Rogers, S. Alan Stern, James M. Stratton, Steven R. Vernon, Stephen P. Williams, The New Horizons Spacecraft; Space Science Reviews Volume 140, Issue 1-4 , pp 23-47 (2007)

(14) Janhunen, P., et al., Invited Article: Electric solar wind sail: Toward test missions," Rev. Sci. Instr. 81, 111301 (2010).

(15) Hoyt, R.P., Forward, R.L., Failure resistant multiline tether, US pat # 6,386,484, May 14, 2002.

(16) Seppänen, et al., "One kilometer (1 km) electric solar wind sail tether produced automatically", AIP Rev. Sci. Instr., 84, 095102 (2013).

(17) Janhunen, P, "ESAIL D3.2.2, Design Description, Main Tether Reel, 30Nov2011, DLR German Aerospace Center, Roland Rosta.

(18) "Interstellar Probe Study Ground Rules & Assumptions (GR&A), Revision 2," NASA MSFC ED04, December 9, 2014.

(19) 20 "Mission Overview," NASA and JHU APL, URL: http://solarprobe.jhuapl.edu/mission/ [cited 1 January 2015].